Available online at www.sciencedirect.com

SCIENCE DIRECT®

Coordination Chemistry Reviews 249 (2005) 2510–2533

COORDINATION CHEMISTRY REVIEWS

www.elsevier.com/locate/ccr

Review

Core modified porphyrins – a macrocyclic platform for organometallic chemistry

Piotr J. Chmielewski*, Lechosław Latos-Grażyński**

Department of Chemistry, University of Wrocław, 14 F. Joliot-Curie Street, 50-383 Wrocław, Poland

Received 8 March 2005; accepted 23 May 2005
Available online 7 July 2005

Contents

Abstract

An alteration of a metalloporphyrin coordination core, exemplified by 21-heteroporphyrins and 2-aza-21-carbaporphyrin (N-confused porphyrin, inverted porphyrin), provides a route of choice to stabilize unusual oxidation states and coordination geometries, affording a stabilization of such rare species as organometallic high-spin nickel(II) or copper(II) derivatives. This review focuses on reactivity and electronic structure of peculiar organometallic compounds trapped due to the appropriate choice of the suitable macrocyclic platform.

Keywords: Porphyrin; Porphyrinoids; Heteroporphyrins; Organometallic chemistry

1. Introduction

Modifications of the porphyrin core involving the introduction of a CH unit or a heteroatom (X = O, S, Se, Te) in place of one of the nitrogen atoms have led to the preparation of a series of carbaporphyrinoids and 21-heteroporphyrins, which have interesting properties both in terms of their aromatic character and their potential ability to bind metal ions [1–4]. Such replacements preserve three regular pyrrole moieties while the (CNNN) or (XNNN) set of donors becomes the denominator of the monocarbaporphyrinoid or 21-heteroporphyrin structure, respectively [5–8].

Carbaporphyrins [5,7], porphyrin analogues with a C–H unit in the coordination core afforded rare organometallic compounds of transition elements, often stabilizing atypical oxidation states or unusual coordination geometries. The stability of these compounds is enhanced by the presence of a carbon donor, favorably oriented in the equatorial plane of the macrocycle. In particular, 5,10,15,20-tetraaryl-2-aza-21-carbaporphyrin NCP (inverted or N-confused porphyrin) [1,2,9], a carbaporphyrinoid of major interest in this contri-

---

* Corresponding author. Tel.: +48 71 37 572 77; fax: +48 71 32 823 48.
** Corresponding author. Tel.: +48 71 37 572 56.
E-mail addresses: pjc@wchuwr.chem.uni.wroc.pl (P.J. Chmielewski), llg@wchuwr.chem.uni.wroc.pl (L. Latos-Grażyński).

0010-8545/$ – see front matter © 2005 Elsevier B.V. All rights reserved.
doi:10.1016/j.ccr.2005.05.015

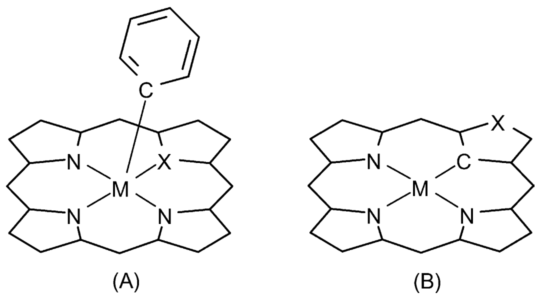

Scheme 1. Organometallic complexes with apical (A) and equatorial (B) location of the M—C bond.

bution, revealed a remarkable tendency to stabilize unique organometallic derivatives [5,7,8,10].

The specialized coordinating core of 21-heteroporphyrins allowed the generation of rare oxidation states of coordinated metal ions and systematic exploration of the coordination modes of five-member heterocycles built into the macrocycle [5]. Significantly for the line of research discussed, five-coordinate metalloheteroporphyrins provide a suitable platform to explore organometallic chemistry with an organometallic bond located in the axial position(s) (Scheme 1A). Such an "axial" approach meaningfully completes the "equatorial" organometallic chemistry of metallocarbaporphyrinoids (Scheme 1B).

Originally our laboratory systematically examined the coordination chemistry of nickel heteroporphyrins [5,11–15]. It was determined that heteroporphyrins stabilize the uncommon nickel(I) oxidation state [11,14]. Once the nickel(II) ion was located in the heteroporphyrin macrocycle the extremely rare high-spin organonickel(II) complexes could be trapped and identified [16–18]. In particular, organometallic chemistry of nickel(II) and stabilization of nickel(I) attracted much attention in light of their biochemical implications. Analogous species have been suggested to participate in the mechanisms of reactions of methyl-S-coenzyme-M reductase [19,20].

It has been well established that 5,10,15,20-tetraarylporphyrins provide a suitable environment for a variety of applications, efficiently controllable by peripheral substitution [21]. Certainly, the core modifications, e.g. in 21-heteroporphyrins and inverted porphyrins, accompanied by appropriate β- and *meso*-substitutions afford a flexible framework to address challenges of organometallic chemistry.

Following the suggestions of the Guest Editor, we intend to present in this contribution the representative line of investigations carried out in our laboratory. Thus in this review we will mostly focus on the reactivity and electronic structure of peculiar organometallic species, which could be trapped thanks to the appropriate choice of a suitable macrocyclic platform. A review addressing mostly the structural aspects of this chemistry is available in the literature [5].

^{1}H NMR spectroscopy was shown to be a definitive method for detecting and characterizing paramagnetic "regular" metalloporphyrins in different coordination/oxidation states [22]. We have methodically explored the relationship between the coordination geometry and isotropic shifts in a class of paramagnetic organometallic complexes formed by inverted porphyrins and 21-heteroporphyrins. The ^{1}H NMR spectroscopy has been applied as a principal method for monitoring reactions of the organometallic derivatives under consideration. As this spectroscopic approach seems to be our signature, our results in this area will be presented in detail in this review.

To account for the current state of studies, this contribution includes three major sections. They report on axial coordination of carbanions, transition metal complexes of the N-confused porphyrin and its derivatives, reactivity which involves N-confused porphyrin (alkylation) and oxygenation, and eventually on the redox properties of selected organometallic species.

2. Axial coordination of carbanions to the metal ions in the heteroporphyrin environment

Heteroporphyrins are a class of macrocyclic compounds structurally related to tetraphenylporphyrin (TPP) H_2, which are characterized by replacing one or more nitrogen atoms of the coordination core by another heteroatom (Scheme 2). Most of our interest has been concentrated on *meso*-aryl substituted heteroporphyrins [12,14,23–26] as well as their transition metal complexes.

The heteroporphyrin metal complexes are useful for pinpointing certain states of metal ions, which are unstable, but can occur in some complex processes, including those of biological importance. Substitution of one of the nitrogen atoms

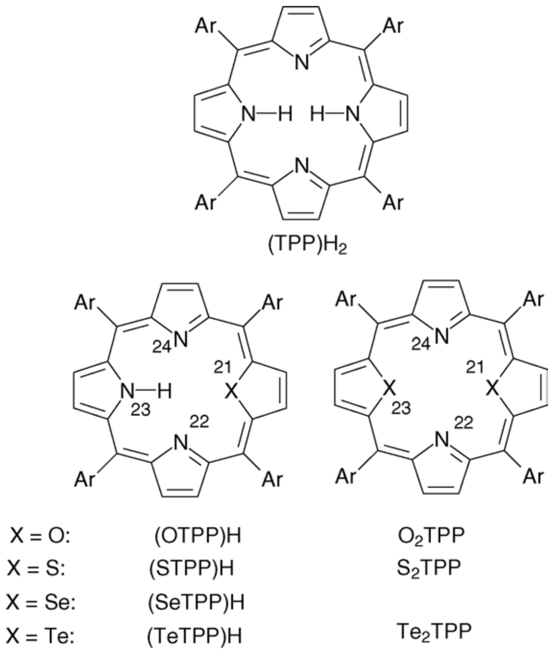

Scheme 2. Regular tetraarylporphyrin and its selected heteroanalogues. The numbering of the coordination sites is given for heteroporphyrins.

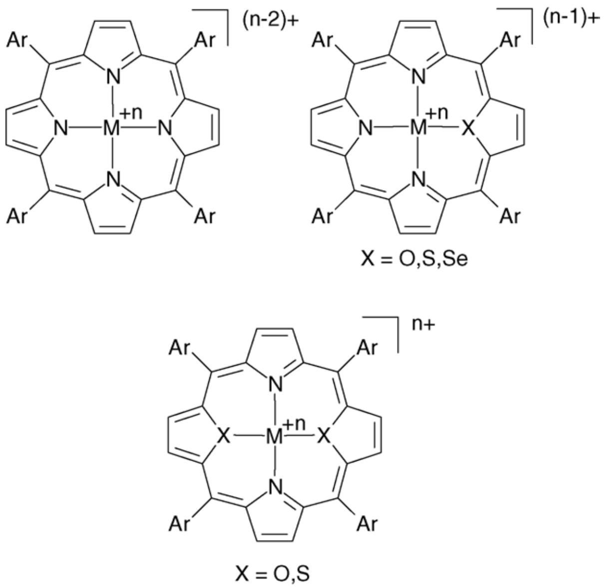

Scheme 3. Neutralization of the charge of a metal cation by porphyrin and its heteroanalogues.

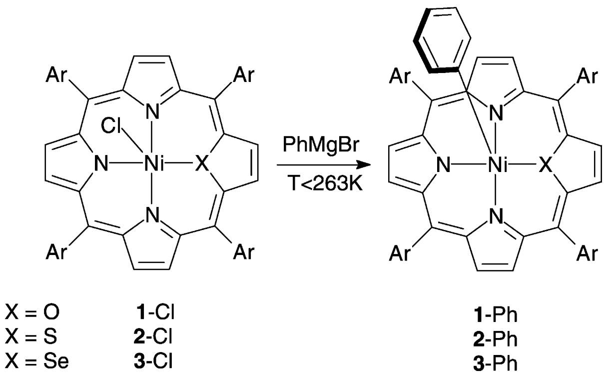

Scheme 4. Formation of organonickel(II) complexes by substitution of an apical ligand.

within the coordination core with another heteroatom results in a significant alteration of the coordination chemistry of the macrocycle. It is not merely a consequence of different donor set but it is also due to a change in a maximum positive charge of the metal ion that can be neutralized by the porphyrin (Scheme 3). Thus, replacing one nitrogen atom with a 16-group element produces a ligand that can be at most monoanionic. In principle such a change can lead to the stabilization of the lower oxidation states of coordinated ions [11,27–29].

Usually the extra positive charge, which is not balanced by the macrocycle, is neutralized, by an anionic ligand coordinated apically to the metal ion. Thus, for divalent metal ions coordination of an anionic axial ligand can be anticipated for metal(II) 21-heteroporphyrins. Obviously, the 21,23-diheteroporphyrins act as neutral ligands. Thus two axial monodentate anionic ligands are necessary to neutralize metal(II) 21,23-diheteroporphyrins. The coordination of trivalent metal ions by 21-heteroporphyrin is typically accompanied by apical coordination of two anions. The halide apical ligands of paramagnetic nickel(II) or iron(III) complexes can be readily exchanged. Thus, a general method of obtaining organometallic complexes is based on replacing an anionic axial ligand by a carbanion, using a Grignard reagent or a lithium aryl or alkyl derivative (Scheme 4).

Originally, we have mainly concentrated on the paramagnetic complexes of nickel(II), for which complexes containing metal–carbon bonds are rare and unstable. The predictable limited stability required the application of low temperatures as well as dry, anaerobic conditions. The method of choice for such studies is ^{1}H NMR spectroscopy. The isotropic shift of the protons localized on the perimeter of the macrocycle, i.e. in the β-positions of the pyrrole and furan, thiophene, or selenophene rings of appropriate (21-XTPP)Ni^{II}Cl is dominated by the contact mechanism involving mainly σ-delocalized spin density with some contribution of the π-delocalization. As a consequence of the dominant role of σ-delocalization all β-H signals are shifted downfield. The deviation of the heterocycle plane from the average plane of the macrocycle makes the delocalization of spin density through the π-bonds more effective. Eventually the net chemical shift of β-protons is negative. This relation between the structure and spectroscopic pattern was confirmed by an X-ray study [14,30].

Once the spectroscopic characterization of paramagnetic chloronickel(II) 21-heteroporphyrins was done for 21-oxa- [14], 21-thia- [30], 21-selena- [25], and 21,23-dioxaporphyrinatonickel(II) [14], ^{1}H NMR spectroscopy could serve as a valuable tool for the identification of related organometallic species. The methodology allows us to recognize the structural alteration that may take place upon ligand exchange. Table 1 contains ^{1}H NMR data for the paramagnetic nickel(II) complexes of 21-oxaporphyrin (OTPP)H, 21,23-dioxaporphyrin O_2TPP, 21-thiaporphyrin (STPP)H, and 21-selenaporphyrin (SeTPP)H with chloride or phenyl as apical ligands. The strong downfield shift of all axial σ-phenyl protons in the monoaryl adducts (21-XTPP)Ni^{II}(Aryl) indicates a mechanism of spin density delocalization involving predominately the σ-framework. The chemical shift attenuates in the order *ortho* > *meta* > *para* which indicates a η^{1}-coordination of the σ-bonded phenyl [17,18]. Considering the relationship between the isotropic shift and geometry of the macrocycle it should be noted that the deformation of the macrocycle changes upon coordination of the phenyl ligand. In particular, the signal of the β-protons of one of the pyrrole is now relocated upfield, reflecting the higher contribution of π-orbitals to the spin-density delocalization, and thus, a strong deviation of this pyrrole ring from an average plane of the coordination core (Scheme 5).

Formation of the bis-σ-aryl adduct of the paramagnetic nickel(II) was anticipated once the hexacoordinated dioxaporphyrin complex (O_2TPP)Ni$^{II}X_2$ (**4**) was used as a substrate. However, the stoichiometry of the adduct depends on the Grignard reagent that is the source of carbanion as well as

Table 1
^{1}H NMR data for nickel(II) complexes of heteroporphyrins

Complex	Pyrrole	Modified ring	Phenyl	Reference
(OTPP)NiCl[a] (**1**-Cl)	57.5, 56.9, 18.1	30.2	–	[14]
(O$_2$TPP)NiCl$_2$[a] (**4**-Cl$_2$)	50.9	37.7	–	[14]
(STPP)NiCl[a] (**2**-Cl)	64.6, 32.5, 30.8	−29.8	–	[30]
(SeTPP)NiCl[a] (**3**-Cl)	68.3, 40.2, 17.1	−38.7	–	[25]
(OTPP)Ni(Ph)[b] (**1**-Ph)	83.7, 62.6, −13.1	30.0	164.7(*m*), 60.2 (*p*)	[17]
(STPP)Ni(Ph)[c] (**2**-Ph)	87.0, 35.4, 2.0	−58.8	616 (*o*), 170 (*m*), 76 (*p*)	[18]
(SeTPP)Ni(Ph)[b] (**3**-Ph)	89.7, 20.8, −15.0	−64.4	151.8 (*m*), 65.8 (*p*)	[17]
(O$_2$TPP)Ni(Ph)Cl[d] (**4**-PhCl)	35.0	28.2	141.05(*m*), 70.01(*p*)	[16]
(O$_2$TPP)Ni(Ph)$_2$[e] (**4**-Ph$_2$)	−143.0	−31.3	5.5(*o*), −4.5(*m*)	[16]

[a] Spectra taken in CDCl$_3$ at 295 K.
[b] Spectra taken in toluene-d$_8$ at 203 K.
[c] Spectra taken in toluene-d$_8$ at 233 K.
[d] Spectra taken in toluene-d$_8$ at 223 K.

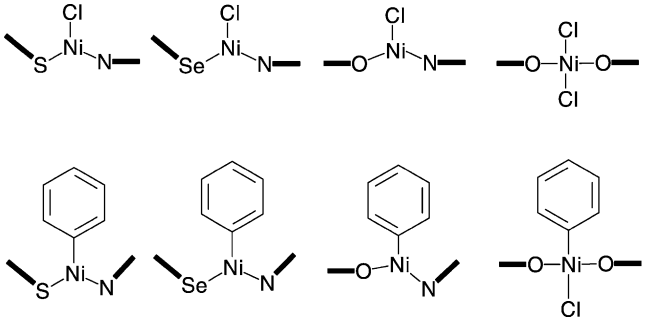

Scheme 5. Deviation from planarity of the coordination core in halide and phenyl heteroporphyrin nickel(II) complexes.

on the axial ligand in the starting compound [16]. The spectroscopic characteristic of the monoadduct (O$_2$TPP)Ni(Ph)Cl (**4**-PhCl) (Scheme 6, Fig. 1A) is similar to those observed for **1**-Ph, **2**-Ph, and **3**-Ph except for the obvious differences due to a different coordination number. On the other hand, the spectroscopic pattern of the diadduct has no precedence among the paramagnetic nickel(II) heteroporphyrins. Both pyrrole and furan proton signals of **4**-Ph$_2$ are strongly shifted upfield, while phenyl protons resonate in the very narrow region (−5 to +9 ppm) (Table 1, Fig. 1B) [16]. Such a profound alteration of the spectroscopic pattern implies severe differences either in the geometry or the electronic state. The *cis*-coordination of the aryl ligands can account for the very high contribution of the nickel d$_\pi$-orbitals in the spin-density delocalization caused by a strong deformation of the macrocycle. Alternatively, reduction of the 21,23-heteroporphyrin by an excess of the Grignard reagent was considered. Consequently the bis-phenyl adduct **4**-Ph$_2$ is expected to contain a 21,23-dioxaporphyrin anion radical with a π-spin density distributed over the equatorial ligand as reflected by peculiar shifts seen in the NMR spectra. In this case two σ-phenyls of **4**-Ph$_2$ are located apically on opposite sides of the macrocycle (Scheme 7).

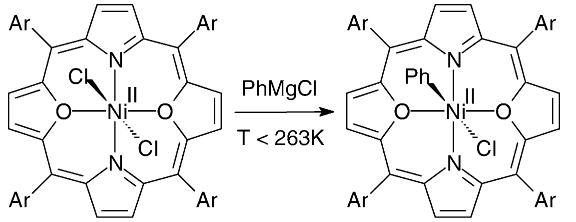

4-Cl$_2$

4-PhCl

Scheme 6. Formation of monoaryl complex of nickel(II) dioxaporphyrin [16].

The thermal decomposition ($t > 10\,^{\circ}$C) of paramagnetic σ-arylnickel(II) heteroporphyrins was related to the homolytic Ni–C bond fission accompanied by reduction of the nickel(II) ion. The decomposition products were detected by EPR (Scheme 8). The spectroscopic parameters found for prod-

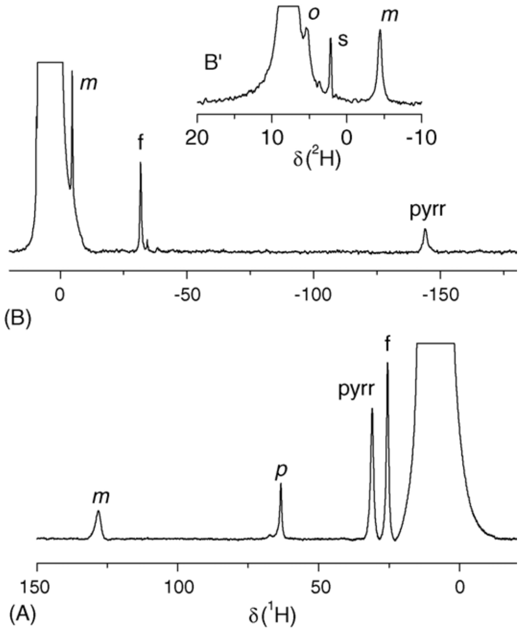

Fig. 1. ^{1}H NMR spectra of phenyl adducts of nickel(II) 21,23-dioxaporphyrin recorded in toluene-d$_8$ at 243 K: (A) monoadduct **4**-PhCl, (B) diadduct **4**-(Ph)$_2$. The ^{2}H NMR spectrum of the diaduct obtained with C$_6$D$_5^-$ in toluene at 243 K is shown in inset (B′) Assignments: pyrr – pyrrole protons, f – furan protons, *o*, *m*, *p* – *ortho*, *meta*, *para* protons (deuterons) of the coordinated phenyl, s – solvent [16].

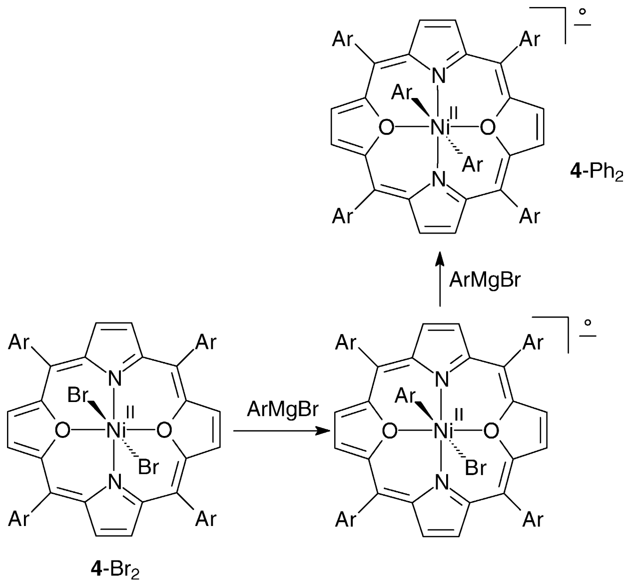

Scheme 7. Proposed reaction path for the formation of the diaryl adduct of the nickel(II) dioxaporphyrin complex [16].

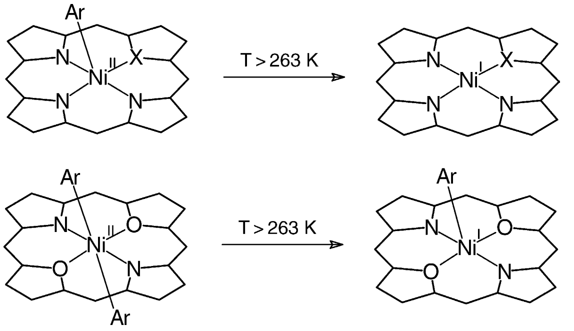

Scheme 8. Formation of nickel(I) complexes from heteroporphyrin nickel(II) aryl adducts.

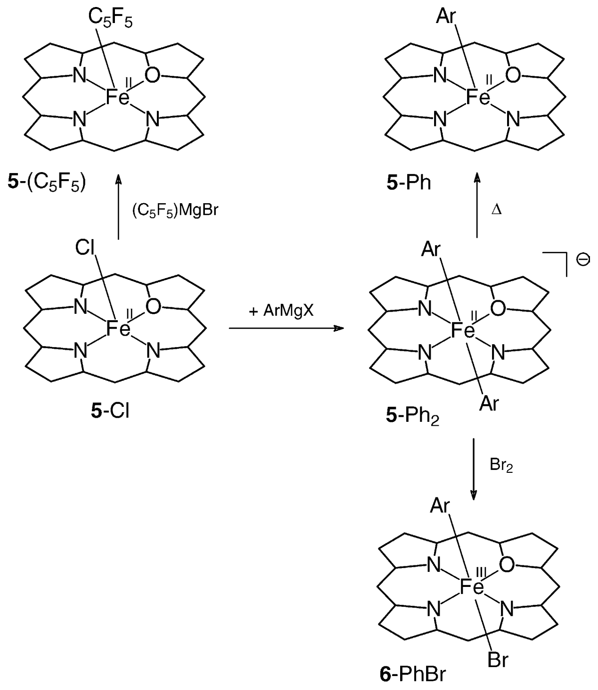

Scheme 9. Formation of aryl adducts of iron(II) 21-oxaporphyrin [31].

ucts of the **1**-Ph, **2**-Ph or **3**-Ph thermal decomposition could be reproduced by one-electron reduction of **1**-Cl, **2**-Cl or **3**-Cl with zinc amalgam [11,14,17,18,29]. It was also demonstrated that the bis-phenyl adduct **4**-Ph$_2$ undergoes the homolytic dissociation of one aryl ligand to yield **4**-Ph which is EPR active. Thus, this process lead to the formation of extremely rare organometallic complex of nickel(I). The existence and nature of **4**-Ph was deduced on the basis of the EPR parameter analysis (Table 2). The EPR data of **4**-Ph are different from those of nickel(I) 21,23-dioxaporphyrins **4**-Cl or **4**-Br produced by one-electron reduction **4**-Cl$_2$ or **4**-Br$_2$ [16]. Remarkably the EPR parameters of **4**-Ph depend also on the carbanion furnished by a Grignard reagent, confirming the aryl coordination to nickel(I).

Table 2
EPR parameters of (O$_2$TPP)Ni^I(Solv)X in frozen toluene solutions at 77 K [16]

X	Solv	g_1	g_2	g_3
Ph$^-$	THF	2.418	2.161	2.049
Ph$^-$	Et$_2$O$_2$	2.343	2.245	2.023
m-Tol$^-$	Et$_2$O	2.326	2.232	2.024
Cl$^-$	–	2.298	2.140	2.093
Br$^-$	–	2.344	2.139	2.086
Br$^-$	THF	2.372	2.138	2.058

Coordination of carbanions by chloroiron(II) oxaporphyrin (OTPP)Fe^{II}Cl (**5**-Cl) was followed by ^{1}H NMR spectroscopy [31]. Addition of (C$_6$F$_5$)MgBr to the toluene solution of **5**-Cl in the absence of dioxygen at 205 K resulted in the formation of the high-spin **5**-(C$_6$F$_5$). Titration of **5**-Cl with PhMgBr (205 K) yielded a rare six-coordinate species which binds two σ-aryl ligands [(OTPP)Fe^{II}(Ph)$_2$]$^-$ (**5**-Ph$_2$). Warming the solution of the latter complex above 270 K results in decomposition to the mono-σ-phenyliron species **5**-PhCl (Scheme 9).

Controlled oxidation of **5**-Ph$_2$ with Br$_2$ affords (OTPP)Fe^{III}(Ph)Br (**6**-PhBr), which demonstrates a typical ^{1}H NMR pattern of low-spin σ-aryl iron(III) porphyrin. The oxidation mechanism considered involves the (OTPP)Fe^{III}(Ph)$_2$ transient species, which is readily reduced to the iron(I) 21-oxaporphyrin, followed by oxidation with Br$_2$ and replacement of one bromide anion by aryl substituent. The peculiar ^{1}H NMR spectroscopic features of bis-aryl adducts (for instance **5**-(*p*-Tol)$_2$, *p*-tolyl: *ortho*, 30.8; *meta*, 53.6; *para*-CH$_3$, 42.1; furan: −16.0; β-H pyrrole: −27.5, −34.3, −41.8 ppm, at 205 K) are without a parallel to any iron(II) porphyrin or heteroporphyrin and indicate a profound alteration of the electronic structure of iron(II) porphyrin upon the coordination of two σ-aryls.

Titration of either iron(II) **5**-Cl or iron(III) **6**-Cl$_2$ complexes with *n*-BuLi (toluene-d$_8$, 205 K) resulted in the formation of the low-spin (OTPP)Fe^{II}(*n*-Bu) (**5**-Bu, Scheme 10).

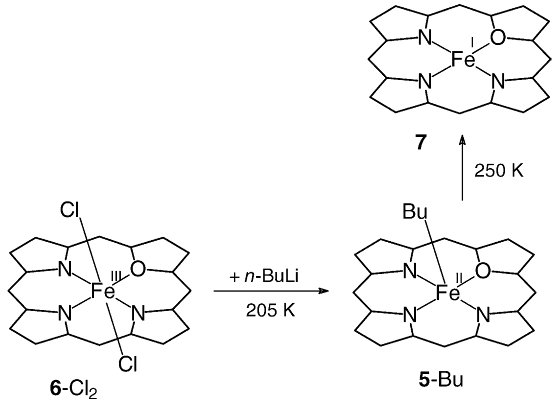

Scheme 10. Butylation and reduction of iron complexes of oxaporphyrin [32].

This compound decomposes via homolytic cleavage of the iron–carbon bond to produce (OTPP)Fe^{I} (**7**). The EPR spectrum of **7** (toluene-d_8, 77 K) is consistent with a predominately d_{z^2} metal orbital contribution to the singly occupied molecular orbital of iron(I) in the oxaporphyrin environment ($g_1 = 2.234$, $g_2 = 2.032$, $g_3 = 1.990$) [32].

In conclusion, the transition metal heteroporphyrin complexes constitute a class of useful systems that can be exploited as models for the spectroscopic identification of unstable organometallic compounds. The special design of the ligand environment allows observation of unusual or transient oxidation and spin states of metal ions.

3. Transition metal complexes of the N-confused porphyrin and its derivatives

2-Aza-21-carbaporphyrin, also called *inverted porphyrin* or *N-confused porphyrin* (hereinafter, NCP, Scheme 11), is an isomer of regular porphyrin characterized by the confusion of one of the pyrrole rings. It plays a particularly important role among porphyrinoids characterized by the presence of a carbon atom within the macrocyclic crevice, including carba- [33–35] and dicarbaporphyrins [36], azuliporphyrin [37–39], *meta*-benziporphyrin [3,40] and its aromatic derivative – oxybenziporphyrin [4], *para*-benziporphyrin [41] or vacataporphyrin [42] (Scheme 12). Nowadays, 10 years after its discovery [1,2,43] this macrocycle is readily obtainable [44] and its coordination chemistry is developing rapidly [8].

Several examples of metal complexes of the other carbon-coordinating porphyrinoids have been reported to date; in particular those of benzi- and oxybenziporphyrins [40,45–48], which have been reviewed recently [49], and of benzocarba-, tropi- and azuliporphyrin [50–54]. Metal complexes have also been characterized for *cis-doubly N-confused* porphyrin (cDNCP) [55,56a,57], *trans-doubly N-confused* porphyrin (*t*DNCP) [56b] and derivatives of *O-confused* oxaporphyrin (OCP) [58]. Coordination chemistry of the other heteroanalogues of NCP (Scheme 11), including *S-confused* thiaporphyrin (SCP) [59], *N-confused* thiaporphyrin (SNCP) [60], or *N-confused* selenaporphyrin (SeNCP) [61] is still awaiting an exploration.

During the past decade our interest in the field was focused on the possibility of stabilization of the uncommon spin and oxidation states of various metal ions forming bond(s) with carbon. The unique reactivity of NCP and its complexes was also a subject of our studies aiming at the synthesis of novel derivatives.

3.1. Charge and the coordination modes of NCP

While the regular porphyrin is invariably a dianionic ligand, the maximum charge of the coordinated metal ion that

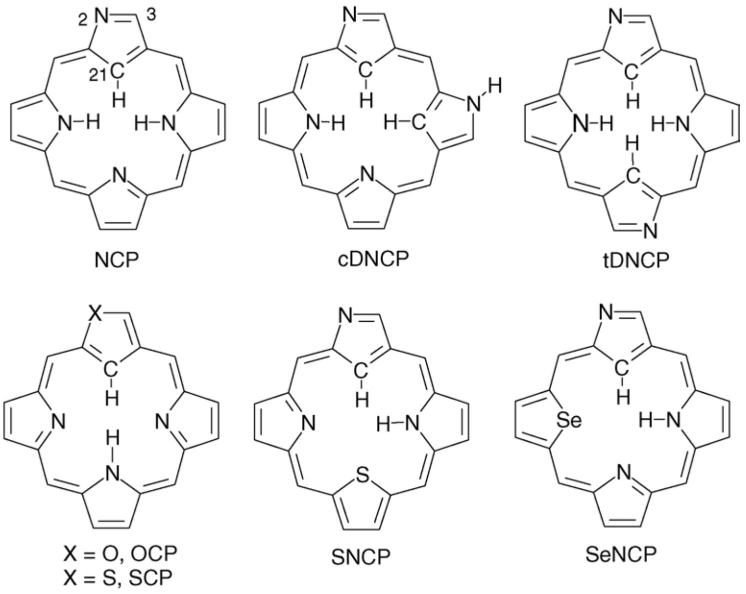

Scheme 11. Skeletons of the *confused* porphyrins and heteroporphyrins.

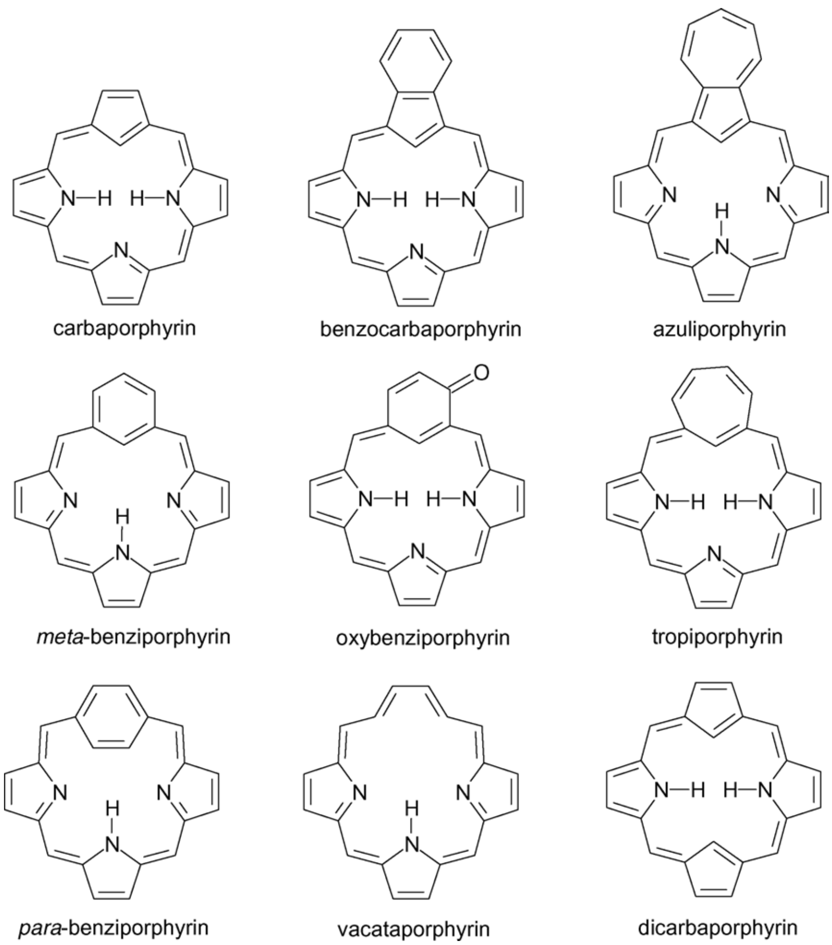

Scheme 12. Skeletons of carbaporphyrinoids.

can be neutralized by the fully deprotonated N-confused porphyrin is +3. However, NCP as a ligand of many faces can act as either trianionic, dianionic, monoanionic, or as a neutral ligand involving all internal donor sites of the macrocyclic crevice – or only some of them (Scheme 13). Also the porphyrin perimeter, in particular the external nitrogen of the *confused* pyrrole, can participate in the coordination. The deprotonation level of NCP in a metal complex depends on

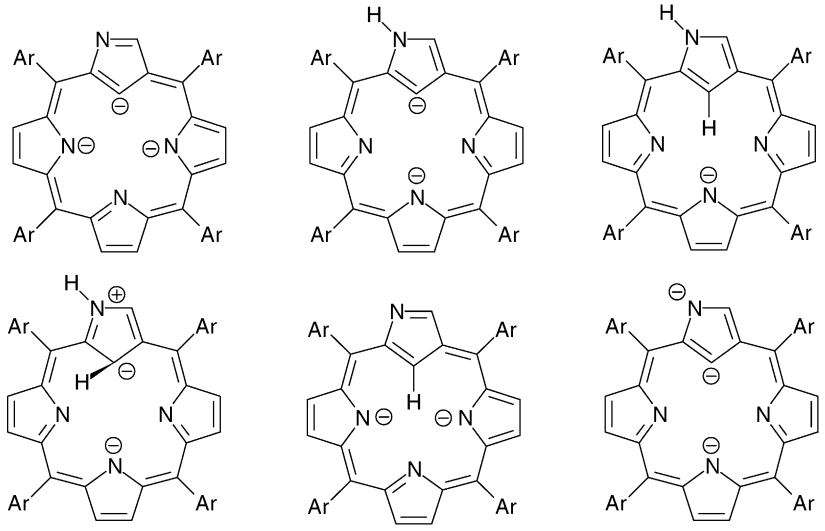

Scheme 13. Distribution of formal charges among the donor sites in the NCP ligand.

the metal ion, mainly on its charge. There is, however, no general correlation between the oxidation state of the metal and the charge of the ligand. Deprotonation of the internal 21-carbon can be identified as a crucial factor determining the total ligand charge. The protonation status of the external nitrogen (hereinafter, 2-N) plays an important role as well, controlling the macrocyclic charge distribution. Eventually, the ligand nature as related to the feasible tautomers of N-confused porphyrin [62,63], can be distinguished by the way in which the internal carbon atom coordinate metal ions (Scheme 14) [64].

In general, there are three different types of coordination observed for the internal carbon (hereinafter C-21) of the *confused* pyrrole (Scheme 14): deprotonated σ-bonding carbanion of sp^2 hybridization (modes **a**–**c**), π side-on coordination of protonated sp^2 atom (modes **d** and **e**), and σ-bonding protonated sp^3 carbanion (mode **f**). In some cases it is possible to change the coordination mode for a given metal ion without changing its spin/oxidation state, merely by addition or abstraction of a proton. In other cases, the oxidation of the metal is not accompanied by proton abstraction.

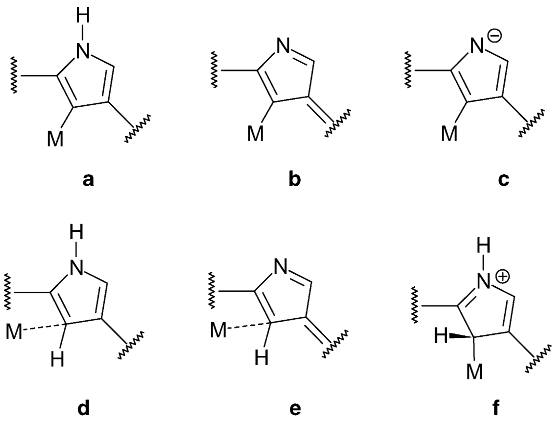

Scheme 14. Coordination modes of the *confused* pyrrole.

It seems natural that in the case of highly charged ions the ligand will adopt a fully deprotonated form, wherein all internal donor sites are involved in coordination. Actually, such an arrangement is observed in the NCP complexes of Mn^{III}, Co^{III}, Cu^{III}, Ag^{III}, and Sb^{V} (Scheme 15) [65–70]. In fact, all known silver complexes of NCP [71] contain the diamagnetic Ag^{III} ion and the ligand is trianionic [68]. The tendency to stabilize this, otherwise unstable oxidation state of silver, seems to be common for the carbon-coordinating macrocycles related to porphyrins [51–53]. The external nitrogen of (NCP)Sb^{V}Br$_2$ can be either unprotonated or protonated, which is reflected by measurable changes in the axial bond distances [70]. Still, in certain systems containing trivalent

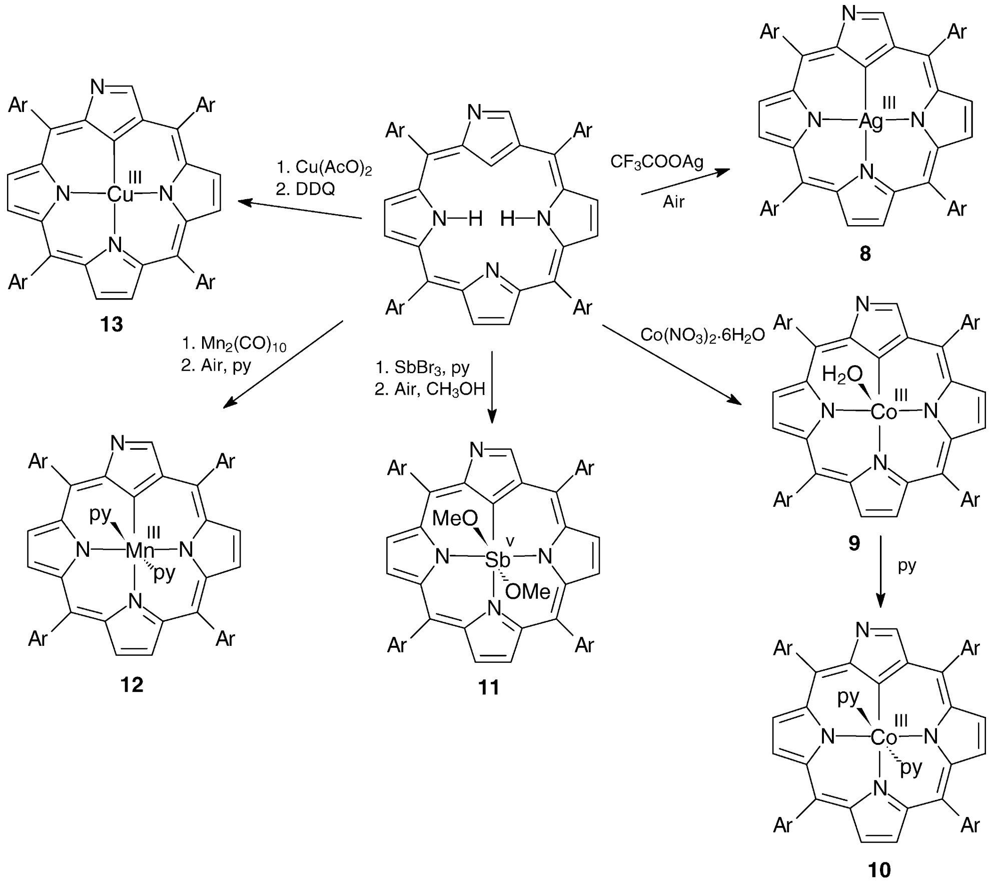

Scheme 15. Formation of NCP metal complexes containing the fully deprotonated ligand.

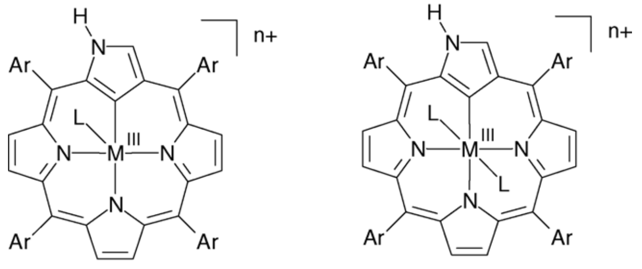

14: M = Mn; L = Br^-, n = 0
15: M = Fe; L = Br^-, n = 0
16: M = Co, L = PPh_3, n = 1
17: M = Ni; L = Br^-, NO_3^-, OH^-; n = 0

15a: M = Fe; L = 1-MeIm, n = 1

Scheme 16. Coordination mode **a** for NCP complexes of trivalent metal ions.

metals, like Mn^{III}, Fe^{III}, Co^{III}, or Ni^{III} ions the NCP acts as a dianion (Scheme 16). Usually, coordination of a counteranion is required. The coordinated anion can be, however, substituted by a neutral ligand [66,72–74]. The form of the complex depends not only on the metal ion type but also on the reaction conditions, i.e. the presence of a proton scavenger, type of oxidant, and available ligands.

Divalent metals of electronic configuration d^8 form diamagnetic neutral NCP complexes (**18**–**21**) with no apical ligand, where 21-C is deprotonated but 2-N bears a proton (Scheme 17) [1,75–77]. The NCP complex of copper(II) (**19**) – the first stable organometallic Cu(II) species – has an analogous structure [78]. The same coordination mode has been observed for nickel(II) complexes of 3-substituted NCP, including a direct linked dimer (**23**) (Fig. 2) [71,79–81].

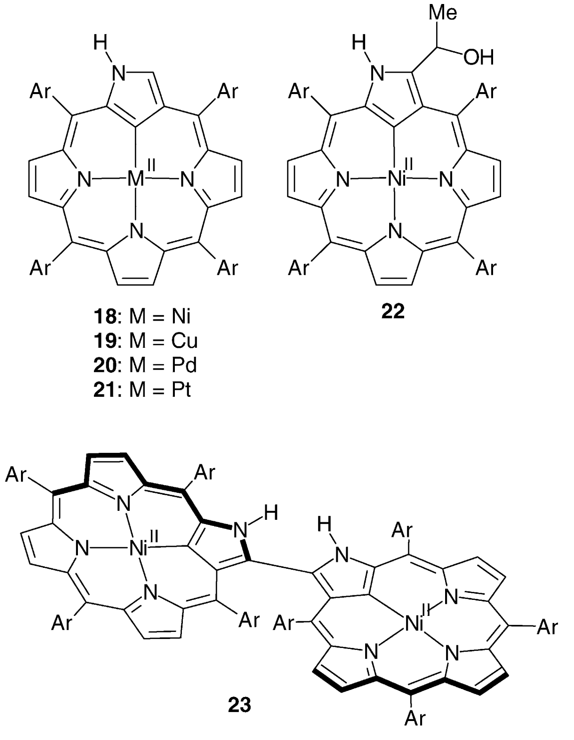

18: M = Ni
19: M = Cu
20: M = Pd
21: M = Pt

22

23

Scheme 17. Divalent metal NCP complexes with coordination mode **a**.

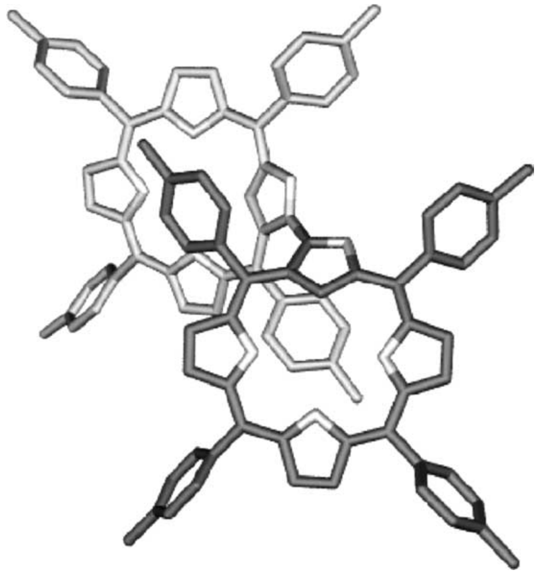

Fig. 2. A wire-frame representation of the molecular structure of a directly linked N-confused diporphyrin $(NCP)_2$ shows lack of rotational freedom around the 3,3′-bond due to the presence of neighboring aryl substituents. All hydrogen atoms are omitted for clarity [81].

The molecules **18**–**21** are effectively planar in the crystal lattice and, due to disorder, they display four-fold pseudosymmetry. In fact they are isostructural with the analogous complexes of the regular *meso*-tetraarylporphyrins. Thus, in most cases the metal–carbon bond could not be identified in the crystal structure.

In solution, the ^1H NMR spectra of NCP complexes, if available, are consistent with low symmetry as each β-H proton contributes with a distinct resonance. The presence of a proton at the external nitrogen of the *confused* pyrrole (2-NH) is also reflected by an appropriate signal. In the ^1H NMR spectrum of $(NCP)Pt^{II}$ (**21**) the satellites due to ^1H-^{195}Pt have been observed for the proton attached to the external carbon of the *confused* pyrrole (3-H) clearly confirming the presence of a platinum(II)–carbon(21) bond (Fig. 3) [77].

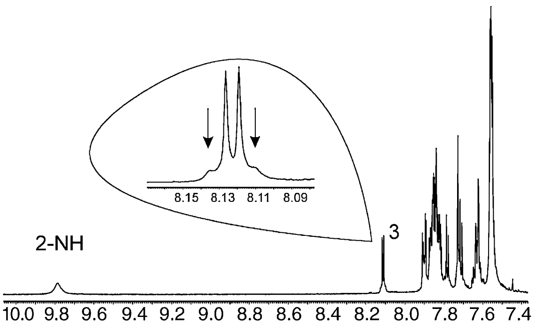

Fig. 3. ^1H NMR spectrum of $(NCP)Pt^{II}$ (**21**) ($CDCl_3$, 323 K). The satellites due to ^1H–^{195}Pt heteronuclear coupling ($^4J_{PtH}$) are marked with arrows on the expansion showing signal of 3-H [77].

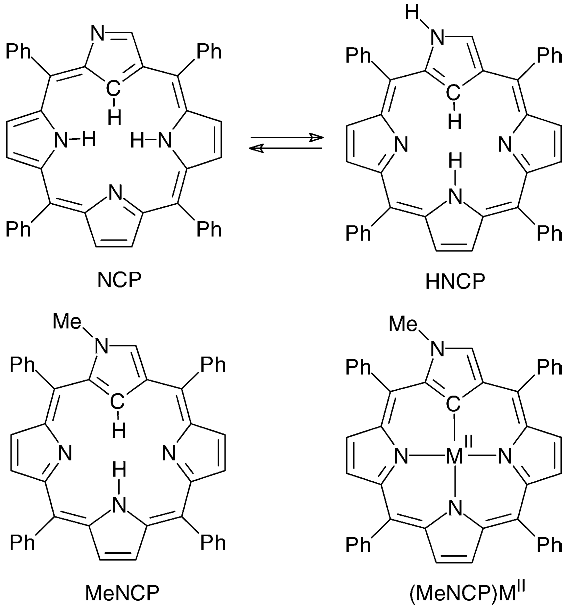

Scheme 18. Preorganization of NCP can be accomplished by tautomeric equilibrium [82] or by alkylation of 2-N [83].

Coordination mode **a** requires a change in the electron density distribution of the ligand relative to the free base. Thus, a tautomeric equilibrium NCP – HNCP that involves proton transfer from the macrocyclic interior to the outer nitrogen has been considered (Scheme 18). In fact, formation of such a tautomeric form is observed in polar solvents [82]. The relative stability of the tautomers as well as carbanionic character of the 21-C in the complexes have been estimated on the basis of DFT calculations [64]. Methylation of NCP readily affords such a preorganized form of the ligand [83]. The spectroscopic characteristics of HNCP and MeNCP are very similar and so are the coordination properties of their macrocyclic interior. Thus MeNCP as well as the other 2-N-substituted derivatives of NCP can be treated as close structural analogues of HNCP as long as the coordination mode is concerned.

Substitution on the external nitrogen is a means to prevent the disorder of the molecules in the solid state. It allows analysis of the metal–carbon bond lengths. In the 2-(2′-bromoethyl)-substituted NCP nickel(II) (**24**) complex the Ni–C21 bond (1.906(4) Å) is shorter than the Ni–N bonds (1.959(3), 1.962(4), 1.964(4)) owing to a smaller radius of the carbanion with respect to the coordinated nitrogen radii (Fig. 4) [84].

The carbanionic character of the coordinated C-21 can be also proven by its nucleophilic properties. In the case of copper(II) [78] and nickel(II) [78,85] complexes the internal carbon of the *confused* pyrrole reversibly accepts a proton. The ^{1}H and ^{13}C NMR-monitored acid titration of (NCP)Ni^{II} (**18**) show the presence of proton located within the aromatic ring and bound to the sp^3-hybridized carbon (Scheme 19). A chiral substituent introduced on the external carbon of the *confused* pyrrole in **22** causes formation of diastereomers

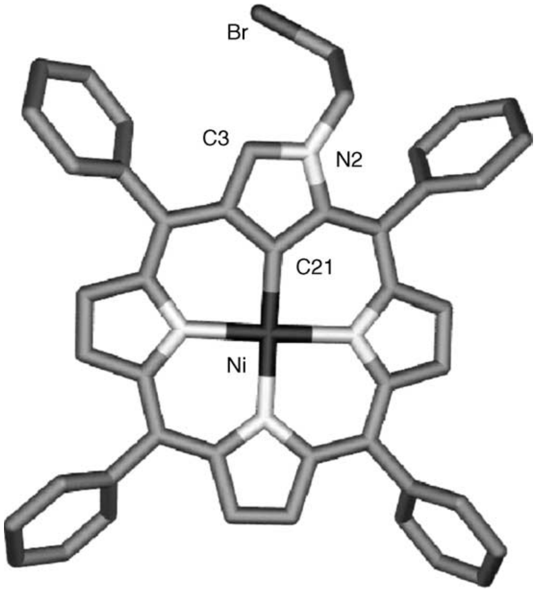

Fig. 4. Molecular structure of 2-(2′-bromoethyl)-5,10,15,20-tetraphenyl-2-aza-21-carbaporphyrinatonickel(II) (**24**). All hydrogen atoms are omitted for clarity [84].

owing to the presence of two centers of asymmetry in the 21-C-protonated species [80].

The effective deprotonation of 2-NH in **18** or **21** requires strong bases as the coordination mode **a** hampers the dissociation of 2-NH due to the carbanionic character of 21-C. The spectrophotometric and ^{1}H NMR titrations of (NCP)Ni^{II} or (NCP)Pt^{II} with potassium *tert*-butoxide (*t*-BuOK) demonstrated stepwise deprotonation of the external nitrogen [77,84]. In the first step the formation of a dimeric species can be deduced on the basis of an upfield shift of the signals of one of the *meso*-aryls. It is in line with the negative-ion mass spectra, which reveal the formation of a potassium-bridged dimer. At higher concentrations of the base a monomeric anionic form dominates (Scheme 20).

In all NCP complexes reported to date that contain divalent ions of manganese, iron, and the 12-group metals the internal carbon of the *confused* pyrrole is protonated (Scheme 21) [65,72,73,86–90]. Both structural and spectroscopic data for zinc complexes show the presence of a proton inside the weakly aromatic macrocycle and sp^2 hybridization of C-21.

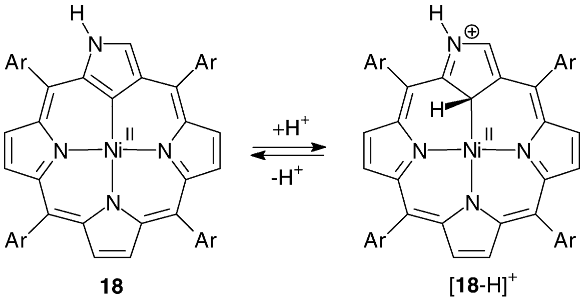

Scheme 19. Reversible protonation of 21-C in (NCP)Ni^{II} [78,85].

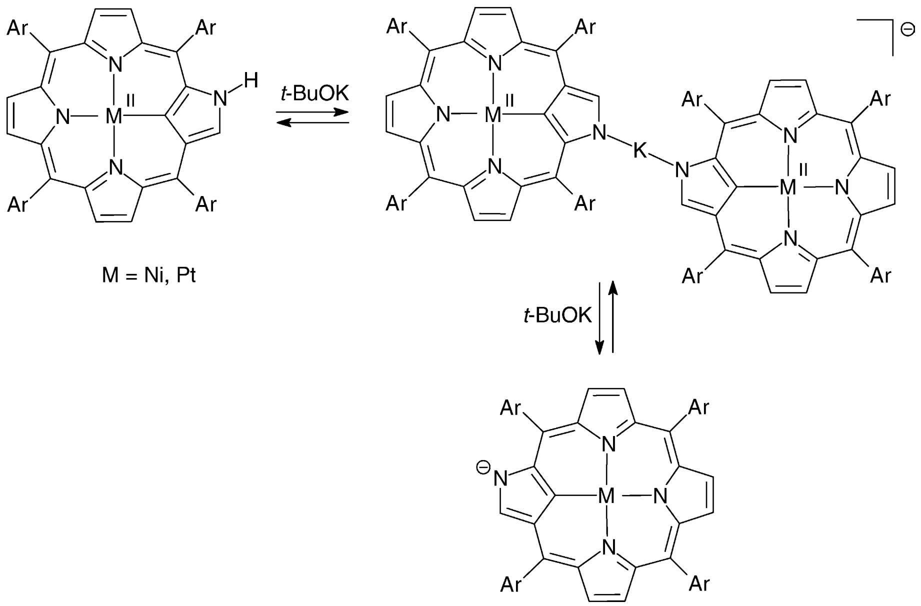

Scheme 20. Deprotonation of 2-NH in complexes with NCP ligand of mode **a** [84].

2-N is also protonated, so that NCP acts as a monoanion [78,91,92]. Application of a proton scavenger removes the proton from the external nitrogen of **25**–**27** converting the ligand into a dianion. This affords either monomers **28**, **29** with an apical neutral ligand or dimeric species **30**–**32** in which deprotonated 2-N is involved in coordination to the metal ion of the other subunit (Scheme 22). Similarly linked heterodimers consisting of subunits with different ions of 12-group elements coordinated by *meso*-diaryl NCP have been reported recently [90]. Application of zinc acetate as a metal source for the insertion results in the formation of another dimeric species (**33**) with two acetate anions and two zinc cations forming a complex bridge between (NCP)Zn subunits (Scheme 23) [91].

The coordination modes **d** and **e** allow a rather weak bonding interaction between metal ion and 21-C considering relevant interatomic distances (2.53(1) and 2.57(1) Å for zinc and cadmium in the dimers, respectively [90], 2.437(7), 2.36(1), and 2.42(1) Å in manganese(II) [72], iron(II) [87], and zinc monomers [91], respectively). Independent insight into such interactions has been provided by ^{1}H NMR spectroscopy. These studies reveal direct coupling between proton attached at 21-C and cadmium or mercury nuclei indicating contact of electron densities localized around the proton and metal in the dimeric complexes [90]. For the monomeric paramagnetic iron(II) complex with an apical bromide ligand an agostic interaction was found on the basis of the structural data [87]. This interaction results in a short distance between iron atom and the proton attached to the 21-C (1.97 Å), and in the remarkably strong downfield shift of 21-H or 21-D (1080–800 ppm at 293 K, depending on the axial ligand choice) in the ^{1}H NMR or ^{2}H NMR spectra (Fig. 5) [89].

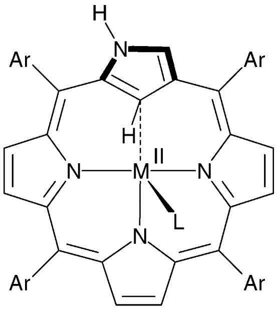

25: M = Mn; L = Br$^-$
26: M = Fe; L = Br$^-$
26a: M = Fe; C$_7$H$_7$S$^-$
27: M = Zn, L = Cl$^-$

Scheme 21. Divalent metal complexes with NCP of coordination mode **d**.

3.2. Reactivity of the NCP metal complexes

Deprotonation of the internal carbon of the *confused* pyrrole in the complexes with coordination mode **a** makes 21-C particularly susceptible for the electrophilic attack [93,94]. Also the external nitrogen can be a target of substitution resulting in complexes similar to **34** particularly under basic conditions. The 21-C-alkylated derivatives (**35a**–**d**) can be efficiently obtained in a reaction of an alkyl halide and a nickel(II) complex of NCP (Scheme 24). A careful choice of a basic catalyst and of the reaction conditions allows for highly selective alkylation of either external nitrogen or internal carbon of the *confused* pyrrole [94]. The alkylation of 21-C with methyl iodide was also observed for the copper(II) complex of NCP [78]. A paramagnetic 2,21-dimethylated derivative **36** can also be obtained efficiently using a large excess of CH$_3$I [94].

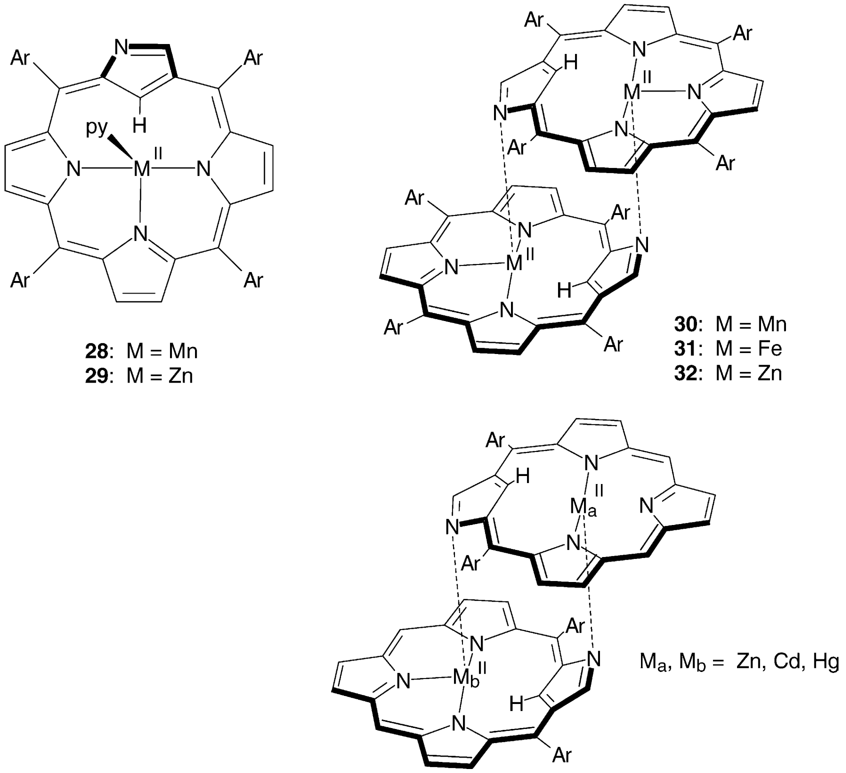

28: M = Mn
29: M = Zn

Scheme 22. Monomeric and dimeric divalent metal complexes with NCP of coordination mode **e**.

Unexpected products **37** and **37a** were obtained in a reaction of (NCP)Ni^{II} with sodium methoxide followed by addition of DDQ which appeared to be a source of cyano group for a process of inner C-cyanide addition [95]. Addition of a methoxy group to the external carbon of the *confused* pyrrole was also observed. In both systems the nickel ion retained its divalent character despite oxidative conditions.

The other way of modification of the macrocyclic perimeter was a Diels–Alder reaction with *o*-benzoquinodimethane, in which **18** acted as a dienophile, yielding nickel(II) N-confused isoquinoporphyrin (**38**) [96].

Oxygenation of the *confused* pyrrole took place when osmium tetraoxide was applied for oxidation of (NCP)Ni^{II} in the presence of pyridine [97]. The EPR and magnetic data unequivocally identified this system as a nickel(III) complex (**39**). The structural parameters revealed coordination of the alkoxide-type oxygen attached to the internal carbon and bonding interaction between metal ion and 21-C which adopted an sp^3 hybridization.

While coordinated to the other redox-active metal ions, the NCP ligand is susceptible to oxygenation on the internal carbon of the *confused* pyrrole. Upon exposure to the

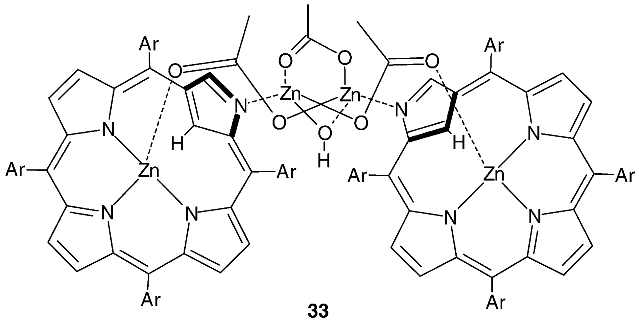

33

Scheme 23. Tetranuclear zinc complex of NCP [91].

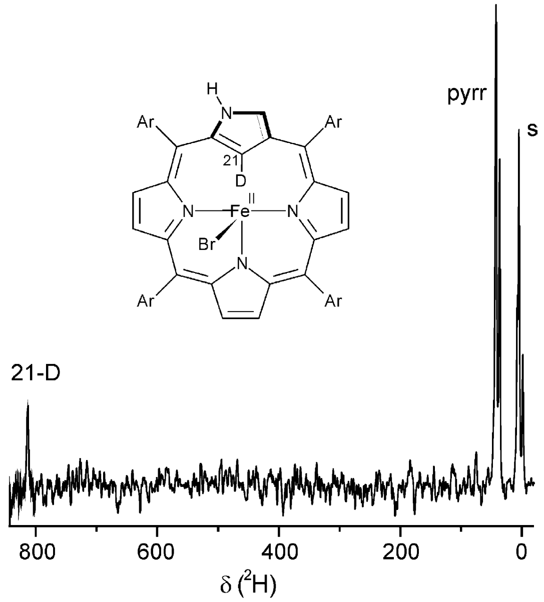

Fig. 5. ^{2}H NMR spectrum of (NCP-d$_8$)Fe^{II}Br (**26**-d$_8$) (all pyrrole protons are replaced by deuterons) in dichloromethane (298 K) [89].

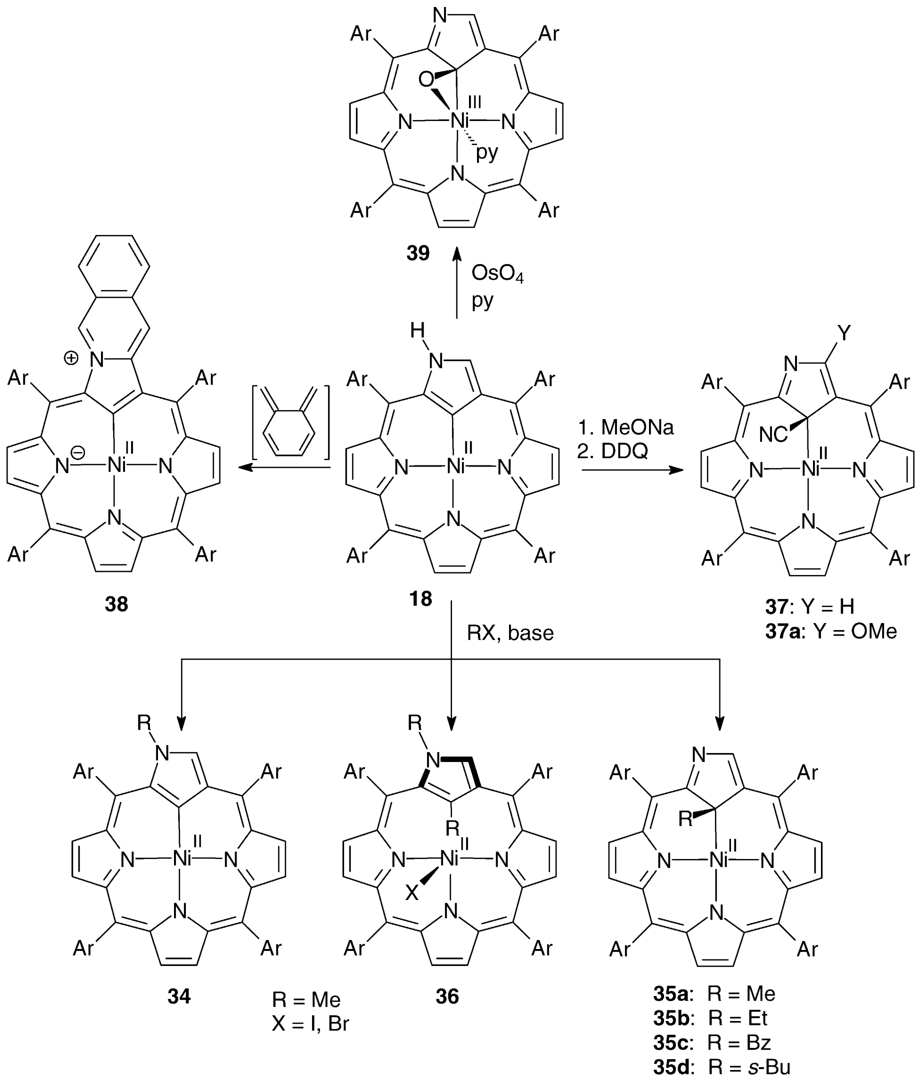

Scheme 24. Reactivity of the *confused* pyrrole in the nickel(II) complex of NCP.

atmospheric oxygen the iron(II) [73] or manganese(II) complexes are converted into their oxo-derivatives (NCPO) and the hydroxylated form of the ligand can be obtained by demetallation [88,98].

Oxidation and oxygenation of (NCP)Fe^{II}Br (**26**) have been followed by ^1H and ^2H NMR spectroscopy (Fig. 6, Scheme 25) [73]. Addition of I_2 or Br_2 to the solution of **26** in the absence of dioxygen results in a one-electron oxidation yielding $[(NCP)Fe^{III}Br]^+$ (**40**) with protonated 21-C. On the other hand, a one-electron oxidation with dioxygen is accompanied by deprotonation of 21-C and formation of an Fe–C bond. Analysis of the ^1H NMR parameters of this oxidation product (β-pyrrole protons 7.2, −10.6, −19.2, −20.6, −23.2, −24.9, −43.2 ppm; 2-NH −76.6 ppm, 298 K) reveals its intermediate spin-state, and five-coordinate environment of the iron(III) which is consistent with its formulation as (NCP)Fe^{III}Br (**15**). In the subsequent step an insertion of the oxygen atom into the Fe^{III}–C bond produce $[(NCPO)Fe^{III}Br]^-$ (**41**). The considered mechanism of (NCP)Fe^{II}Br oxygenation involves the insertion of dioxygen into the Fe–C bond. In the solid state (Fig. 7) in (NCP)Fe^{III}Br (**15**) the iron(III) is five-coordinate with bonds to three pyrrole nitrogen atoms (Fe–N distances: 1.985(8), 2.045(7), 2.023(8) Å), and the pyrrolic trigonal carbon (Fe–C: 1.981(8) Å) whilst in (NCPO)Fe^{III}Br (**42**) the iron(III) forms bonds to three pyrrole nitrogen atoms (Fe–N distances 2.104(5), 2.046(5), 2.102(5) Å), oxygen (2.041(5) Å) and 21-C (2.192(5) Å). Such a geometry suggests a direct interaction between the iron center and the π electron density on the carbonyl group in a η^2 fashion.

The reactivity of positions 2 and 21 in the nickel(II) complex of NCP toward electrophiles can be exploited in the preparation of covalently linked oligomers built from modified N-confused porphyrin subunits (Scheme 26). A variety of monomeric and dimeric products were obtained in the reactions of **18** with dihaloalkanes in the presence of proton scavengers [84,99]. Dihalomethanes yielded the 2,21′-methylene-linked dimer **43** as the major product accom-

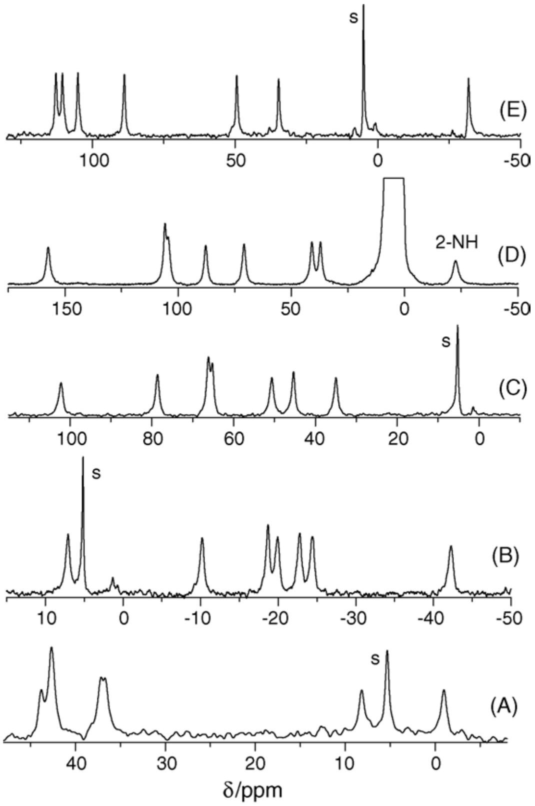

Fig. 6. NMR spectra of iron N-confused porphyrin presenting the β-H or β-D pyrrole and 2-NH resonances: (A) (NCP-d_8)Fe^{II}Br (**26**), 298 K; (B) (NCP-d_7)Fe^{III}Br (**15**), 298 K, ^{2}H NMR; (C) $[(NCPO\text{-}d_7)Fe^{III}Br]^-$ (**41**), 298 K, ^{2}H NMR; (D) (NCPO-d_{20})Fe^{III}Br (**42**), 223 K (^{1}H NMR); (E) $[(NCP\text{-}d_8)Fe^{III}Br]^+$ (**40**), 298 K ^{2}H NMR. The solvent signals are assigned s. NCP-d_8 – selectively deuterated in all pyrrole positions, NCP-d_{20} – selectively deuterated in all *meso*-phenyl positions, A, B, C, E – ^{2}H NMR, in dichloromethane, D – ^{1}H NMR, in dichloromethane-d_2 [73].

panied by a small amount of 2,2′-methylenebis(2-aza-21-carbaporphyrinatonickel(II)) **44** [99]. In the presence of alcohol the dimerization is effectively quenched owing to a Williamson-type reaction of the "free end" of the halomethyl substituent with a nucleophilic alkoxy group that gives 2- or 21-ethoxyethyl-substituted monomers **45**, **46** [84]. A 21,21′-ethylene-linked dimer **47** was obtained in a reaction of (NCP)Ni^{II} with dibromoethane in the presence of potassium carbonate in CH_2Cl_2/ethanol while the 2-bromoethyl-substituted complex **24** was solely formed in THF in the presence of potassium *tert*-butoxide. Under strongly basic conditions the reaction of **18** with 1,3-dibromopropane yielded 21-allyl-substituted monomer (**48**) as the only product [84].

3.3. Charge, coordination modes and nucleophilic properties of the alkylated NCP in its metal complexes

Alkylation of NCP either at the external nitrogen or at the inner carbon of the *confused* pyrrole reduces the maximum negative charge available for the ligand (Scheme 27). Thus, while the unsubstituted NCP is potentially trianionic, the 2- or 21-substituted-derivative can be at most dianionic, and 2,21-disubstituted macrocycle can only be monoanionic, as it contains only one removable proton within the coordination core. The complexes formed by 2-N-substituted ligands lack the possibility to change a status of the external nitrogen upon coordination. As a consequence of this, the coordination mode that can be adopted by the ligand is restricted to the analogoues of modes **a**, **d**, or **f**, whilst the 2,21-dialkylated ligands invariably forms complexes with coordination mode **d** (Scheme 14). The 21-substituted ligands can adopt two different coordination modes. One of them, with no proton on the external nitrogen of the *confused* pyrrole and sp^3 hybridization of the coordinated carbon, occurring in **35**, has no parallel among coordination modes in the metal complexes of the unsubstituted NCP characterized to date. The pyramidal hybridization of 21-C in the internally alkylated complexes is a source of their chirality, which can be infer on the basis of diastereotopic differentiation of the signals of mthylene substituents in ^{1}H NMR spectra of **35b** and **35c**. Moreover, formation of diastereomers is observed in the case of chiral substituents at 21-C in **35d** or for the 21,21′-linked dimer [84,94] (**47**) owing to the presence of two chiral centers.

The carbanionic character of the coordinated internal carbon in the 2-N-alkylated nickel(II) or copper(II) complexes can be deduced on the basis of the nucleophilic character

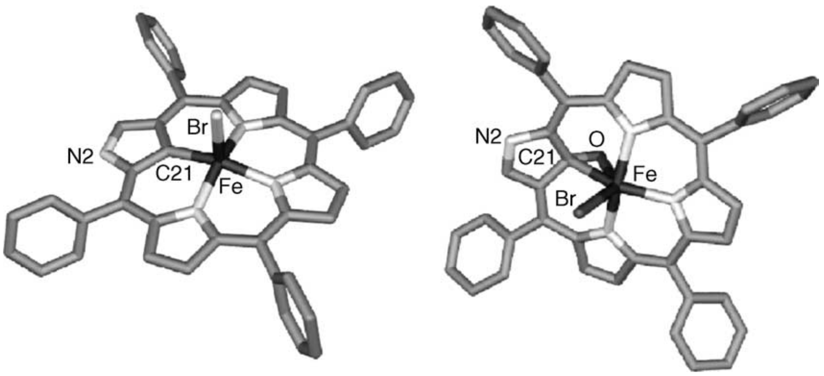

Fig. 7. Molecular structures of (NCP)Fe^{III}Br (**15**) (left) and (NCPO)Fe^{III}Br (**42**) (right). All hydrogens are omitted for clarity, but in both molecules 2-N is protonated [73].

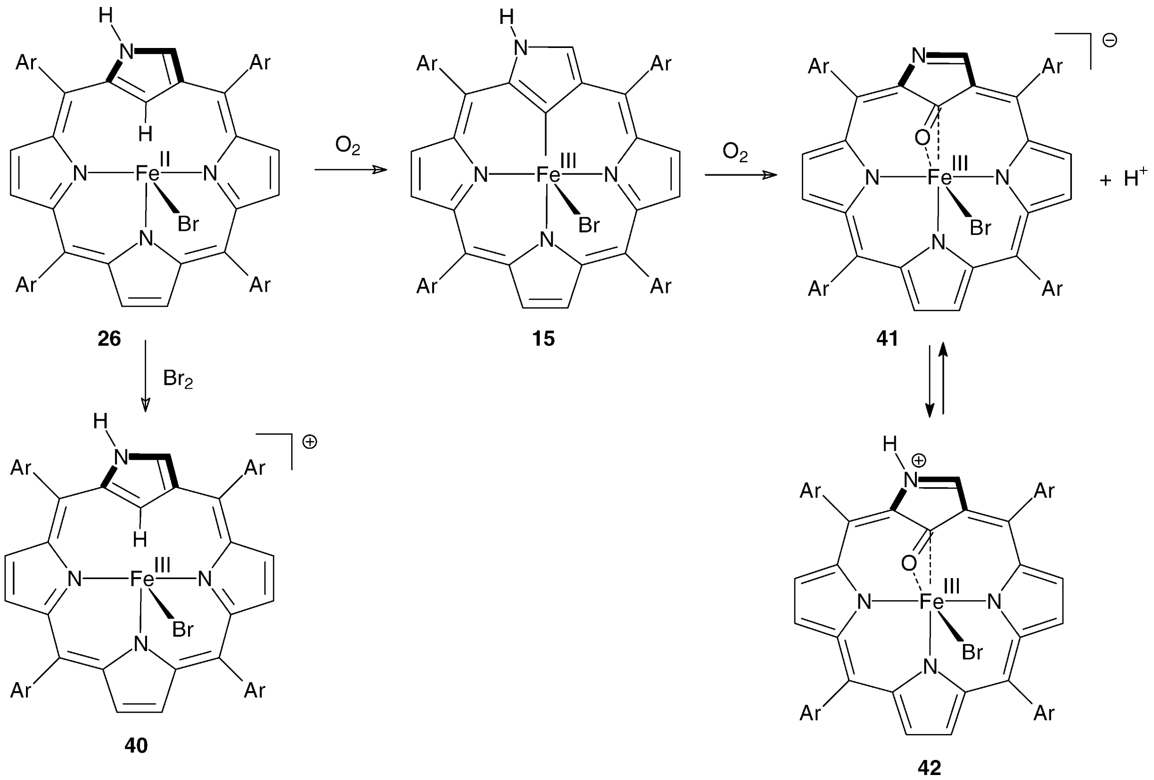

Scheme 25. Oxidation and oxygenation of (NCP)Fe^{II}Br (**26**) [73].

of 21-C (Scheme 28) [78,94]. For the 2-N-methylated NCP copper(II) complex (**49**) acidification of the solution with TFA produces significant spectroscopic changes which can be ascribed to the protonation of the internal carbon (Fig. 8). Addition of the chloride results in a further alteration of the spectrum reflecting the coordination of an anionic ligand. The resulting spin-hamiltonian parameters closely resemble those of the 2,21-dimethylated NCP complex (**50**), strongly suggesting similar local environment of the copper(II) ion.

The protonation of C-21 in nickel(II) species induces chirality. Diastereotopic differentiation of protons can be observed in the ^{1}H NMR spectra for the systems containing methylene groups (**24**, **45**) upon addition of an acid. This is in line with a pyramidal hybridization of 21-C in the protonated complexes. The ^{13}C NMR chemical shift of the internal carbon in these systems (about 40 ppm) is typical of the sp^3 carbon atoms. Most significantly, the protonated complexes remain diamagnetic which indicates a square-planar geometry of the local environment of the metal ion. It also implies lack of any anionic ligand that may be coordinated to the nickel(II), neutralizing the additional positive charge introduced by the proton and changing the spin state [94]. Addition of chloride or application of hydrochloric acid in the place of TFA do not change the spin state of the complex. Clearly, the tendency to coordinate an axial ligand is weaker for nickel(II) than for copper(II) in the same macrocyclic environment.

Formally analogous to the protonation process, methylation of **34** leads to the formation of paramagnetic species **36** in which the metal ion adopts a distorted square-pyramidal geometry and sp^2-hybridized 21-C is weakly side-on π-bonded (Scheme 28) [93]. A singlet–triplet spin equilibrium for the ground state of the nickel(II) is observed upon protonation of the external nitrogen in the 21-monoalkylated complexes [93,94,99] which is accompanied with coordination of the anionic ligand to the metal ion after addition of an acid (Scheme 28). The difference in the spin states of the formally analogous, externally N- and internally C-alkylated nickel(II) complexes, which is induced upon protonation can be accounted for by a stronger tendency of the metal ion in the 21-C alkylated complexes to adopt a distorted geometry of the local environment which seems to be a prerequisite for coordination of an apical ligand. Owing to non-planar geometry of the complex the molecule is chiral after protonation despite the absence of an asymmetric carbon (Scheme 29). A very strong diastereotopic differentiation of the isotropic shift of the signals of methylene protons of the substituent bound to 21-C (e.g. in **35c**-HCl) as well as the formation of diastereomers for systems with chiral substituents (e.g. for **35d**-HCl) are observed in the ^{1}H NMR spectra of these paramagnetic complexes (Fig. 9) [94].

Activation of the carbon–carbon bond in protonated nickel complexes was observed for some substituents attached to 21-C (e.g. for benzyl, ethoxymethyl, and allyl in **35c**-HCl, **46**-HCl, and **48**-HCl, respectively). The oxidative dealkylation of benzyl-substituted complex (**35c**) upon protonation in the presence of air results in the formation of benzaldehyde and

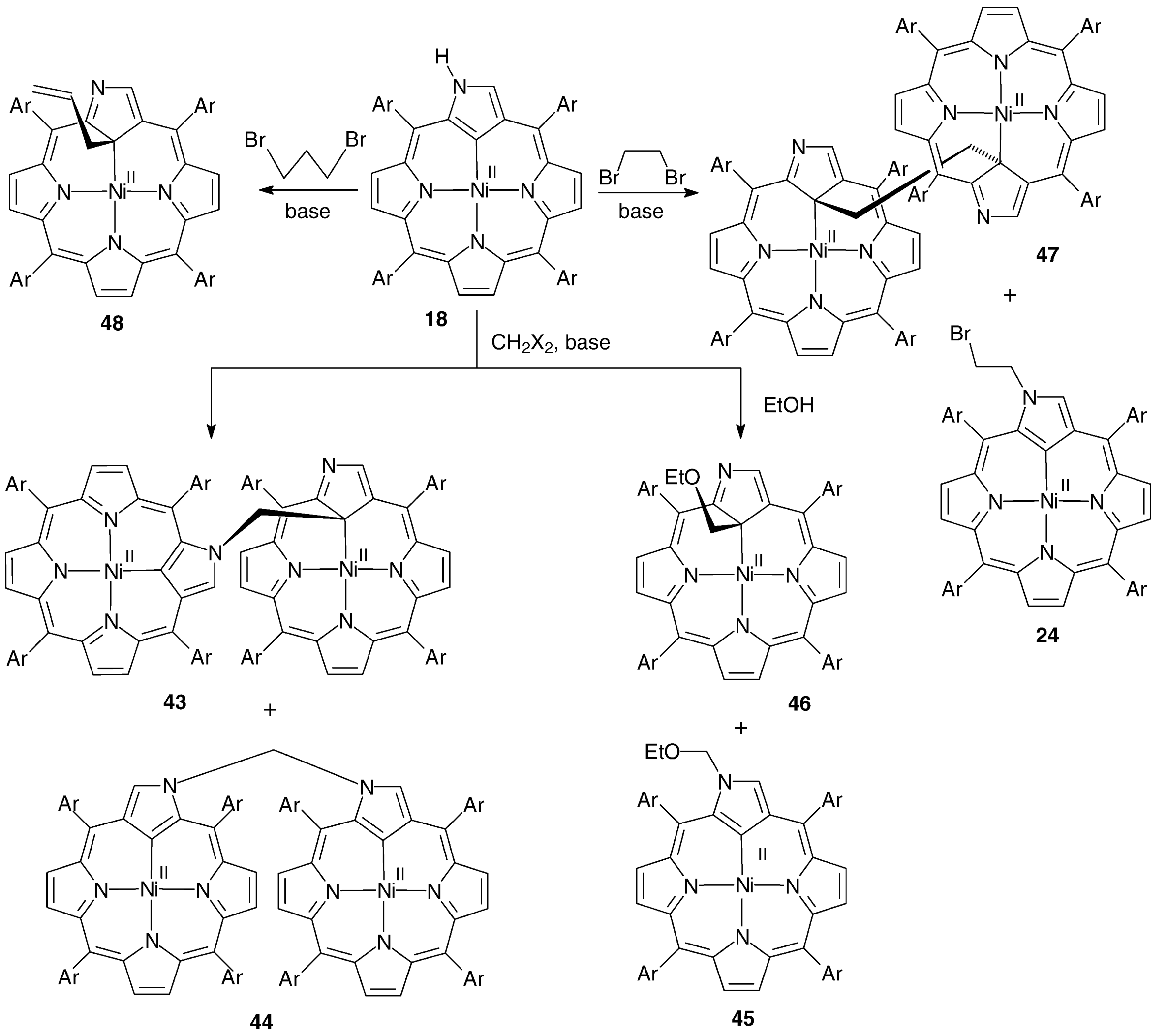

Scheme 26. Reactivity of (NCP)Ni^{II} (**18**) toward dihaloalkanes [84,99].

recovery of the unsubstituted (NCP)Ni^{II} (**18**) (Scheme 30) [94].

Protonation of the external nitrogen of the *confused* pyrrole in the 21-alkylated nickel(II) complexes indicates its nucleophilic character and thus, the outer nitrogen should be a convenient coordination site. Indeed, the reaction of 21-alkylated nickel(II) complexes with $PtCl_2$ in refluxing chloroform yields platinum(II) species containing two porphyrin subunits per molecule (Scheme 31) [77]. The dimer is asymmetric, i.e. the subunits coordinate platinum ion in different ways – one with its external nitrogen, and the other with the external nitrogen and the *ortho*-carbon of the neighboring *meso*-aryl ring (Fig. 10). A similar type of coordination of the platinum(II) [76] and palladium(II) [75] ions was observed for an unsubstituted and non-metalated NCP. In the case of $(NCP)_2Pt^{II}Cl$ both *trans* and *cis*-complexes are formed with some admixture of the monomeric (NCP)Pt^{II} (**21**) containing platinum(II) ion within the macrocyclic core. For the alkylated nickel(II) complexes the *cis*-configuration is observed in the square-planar platinum(II) complexes (**51a**,**b**). Both nickel(II) ions remain in the singlet spin state since their first coordination sphere is roughly square-planar. This is because the additional positive charge introduced by the platinum(II) ion is neutralized by a chloride and by orthometalation. Thus, there is no driving force for the coordination of an anionic ligand to the nickel(II) center(s). In addition to the chemoselectivity, the formation of the dimer is stereoselective. The presence of two stereogenic centers implies the formation of diastereoisomers: one with the same configuration of C-21 on both subunits (mixture of enantiomers), and the other with different configurations. Owing to the steric factors imposed by the neighboring *meso*-aryl rings, only the latter diastereoisomer is present in the reaction mixture, as was determined on the basis of a single crystal X-ray structure and the NMR study in solution [77]. In this platinum(II)-linked dimer both coordination sites of the *confused* pyrroles, i.e. internal carbon and the external nitrogen, are involved in σ-coordination. In other metal complexes of NCP or its derivatives characterized to date, including homo- and heterodimers [65,75,76,86,88,90,91], coordination of the external nitrogen

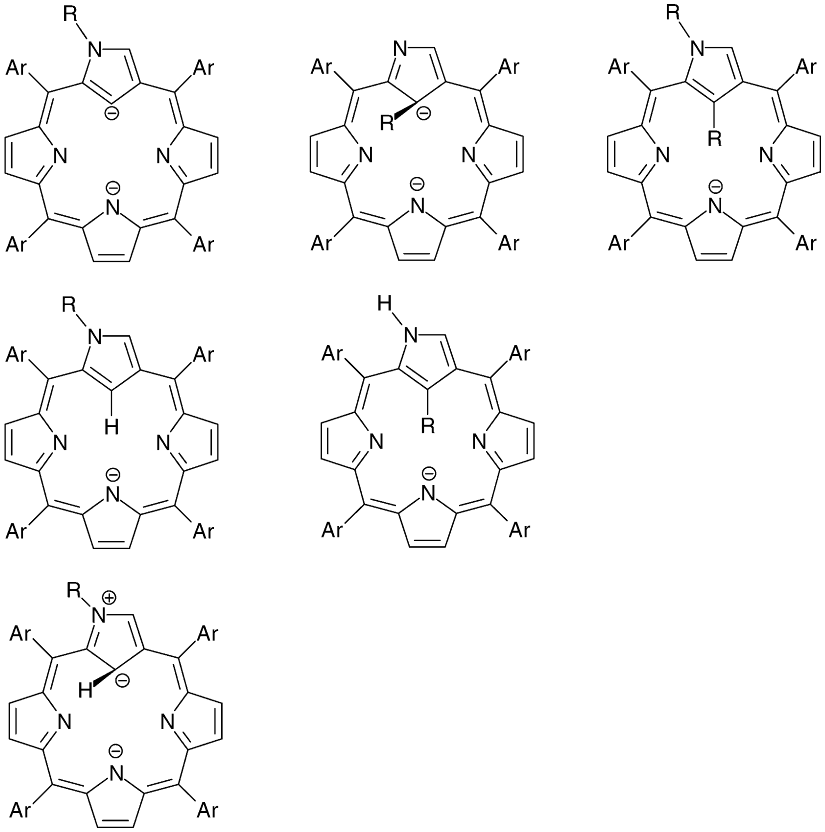

Scheme 27. Coordination modes of alkylated NCP derivatives.

was accompanied either with lack of any coordination via 21-C [56,76,100] or only weak side-on π-bonding with a possible agostic interaction [88].

3.4. *Paramagnetic nickel(II) complex with two different metal–carbon bonds*

The inherent monoanionic character of the 2,21-dimethylated NCP derivative **36** enables the preparation of a paramagnetic nickel(II) complex with two different metal–carbon bonds (one axial and one equatorial) by a simple exchange of the apical chloride (Scheme 32) [101]. Addition of a phenyl Grignard reagent to a toluene solution of the **36** at 203 K results in the formation of a paramagnetic (σ-phenyl)nickel(II) species (**52**). The coordination of the σ-phenyl in **52** is determined by a unique pattern of three σ-phenyl resonances (*ortho* 375.0 ppm; *meta* 108.94 ppm; *para* 35.68 ppm at 283 K) in the ^{1}H NMR and ^{2}H NMR spectra. The high-spin ground electronic state of the phenyl complex is confirmed by the similarity of its NMR spectra to those of the (σ-phenyl)nickel(II) complexes of the 21-heteroporphyrins (Table 1) [16–18]. Titration of **36** with phenyllithium also produces **52**, but simultaneously, a one-electron reduction with excess of PhLi yields **53**. The latter system can be generated by independent routes, e.g., by reduction of the phenylated complex using lithium triethylborohydride or tetrabutylammonium borohydride. The spectroscopic data indicate that the one-electron reduction proceeds without any substantial disruption of the molecular geometry. The presence of two paramagnetic centers in **53**, i.e. the high-spin nickel(II) and the carbaporphyrin anion radical, produces remarkable alteration in the spectroscopic pattern, such as the upfield positions of some β-pyrrole signals and sign alternations of the isotropic shift of the remarkably shifted *meso*-phenyl resonances.

Warming of the phenyl adducts results in the disruption of the nickel-apical carbon bond via homolytic/heterolytic cleavage (Scheme 32). The process yields a mixture of two compounds, which are detected by EPR spectroscopy, both demonstrating a high anisotropy of the **g** tensor in frozen toluene solution at 77 K. One of them (**54**) with $g_1 = 2.237$, $g_2 = 2.092$, and $g_3 = 2.090$ can be described as a nickel(I) complex of the 2,21-dimetylated NCP, while the spin-hamiltonian parameters of the other ($g_1 = 2.115$, $g_2 = 2.030$, $g_3 = 1.940$) suggests concomitant reduction of both metal and the ligand (**55**).

4. Redox properties

Although, at present, studies of the redox properties of metal complexes of NCP and its derivatives are far from complete, some conclusions regarding the relationships between

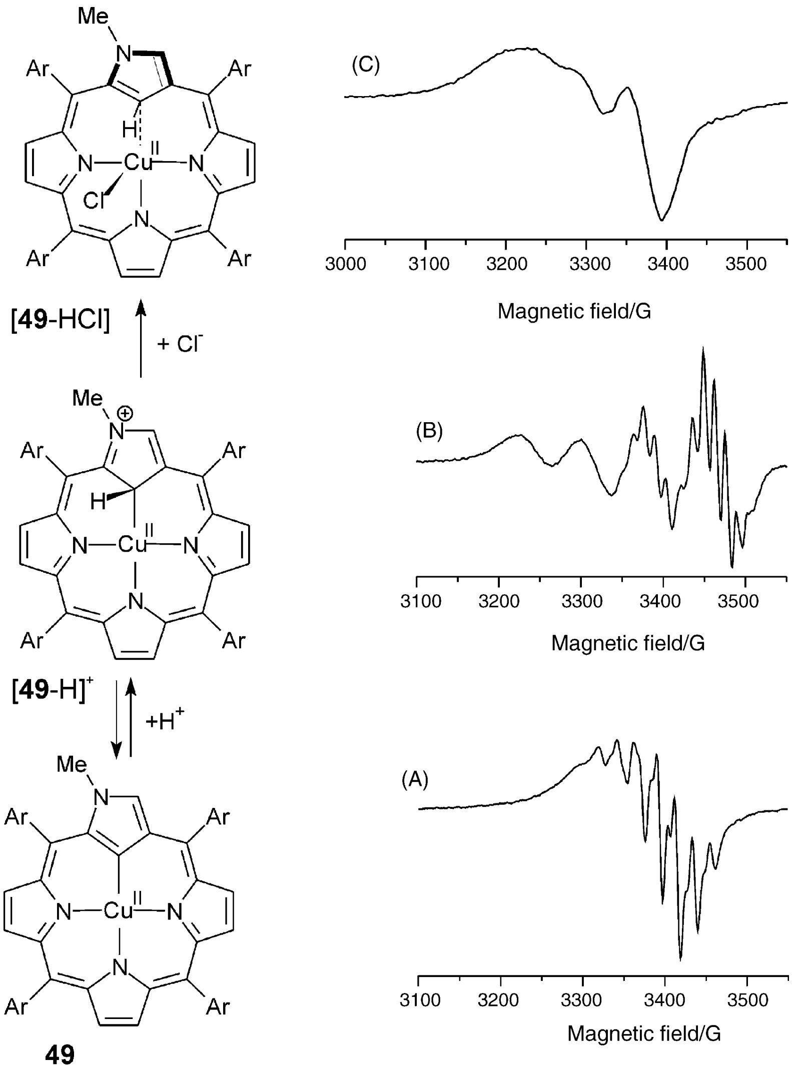

Fig. 8. The EPR spectroscopic changes upon acidification of (MeNCP)Cu^{II} (**49**) with TFA and addition of triethylammonium chloride. Starting from the bottom are shown the isotropic spectra of **49** (trace A), [**49**-H]$^+$ (trace B), [**49**-HCl] (trace C) in dichloromethane (293 K). Microwave frequency 9.788 GHz; microwave power 10 mW, modulation amplitude, 0.6 mT; modulation frequency 100 kHz [78].

the coordination mode and oxidation state can be drawn. For instance, a high stability of the trivalent silver in the environment of the fully deprotonated NCP is reflected by its very wide HOMO–LUMO gap, estimated qualitatively by the difference of redox potentials between the first oxidation and first reduction process [68]. The first oxidation and reduction potentials, observed in the cyclic voltammogram of (NCP)Ag^{III} (**8**) and their separation ($\Delta E = 1.93$ V), suggest a ligand-centered electron transfer.

The electrochemical measurements for nickel(II) and copper(II) complexes of NCP (**18**, **19**) as well as its 2-methylated derivatives (**34**, **49**) indicate a possible metal-center oxidation of the system. Comparison of the first oxidation potentials for these metal ions clearly shows a higher stability of divalent nickel than divalent copper in the NCP environment since the first oxidation potential is about 300 mV higher for nickel(II) than for copper(II) complexes and first reduction potentials are similar [74,78]. Methylation of the external nitrogen does not reduce the tendency of both metals to be oxidized, despite changes in the available maximum charge of metal cation that can be stabilized by the ligand. On the other hand, a strong anodic shift (370 mV) of the first oxidation couple with respect to that of **49** can be observed for a 2,21-dimethylated complex of Cu^{II}, **50**. For the latter system a reversible reduction couple at −224 mV (THF versus SCE) indicates stabilization of monovalent copper in the environment of the monoanionic ligand [78].

Lack of significant influence of 2-N-methylation on the oxidation potential of the divalent ions is related to the fact that the external nitrogen is occupied (by proton or methyl group) both in the reduced and in the oxidized states, and the coordination mode of the *confused* pyrrole is the same (mode **a**). However, upon application of a strong non-coordinating base (e.g. potassium *tert*-butoxide) a significant cathodic shift of about 400 mV is observed for nickel(II) [94] and platinum(II) [77] complexes of NCP (Scheme 33). For the latter

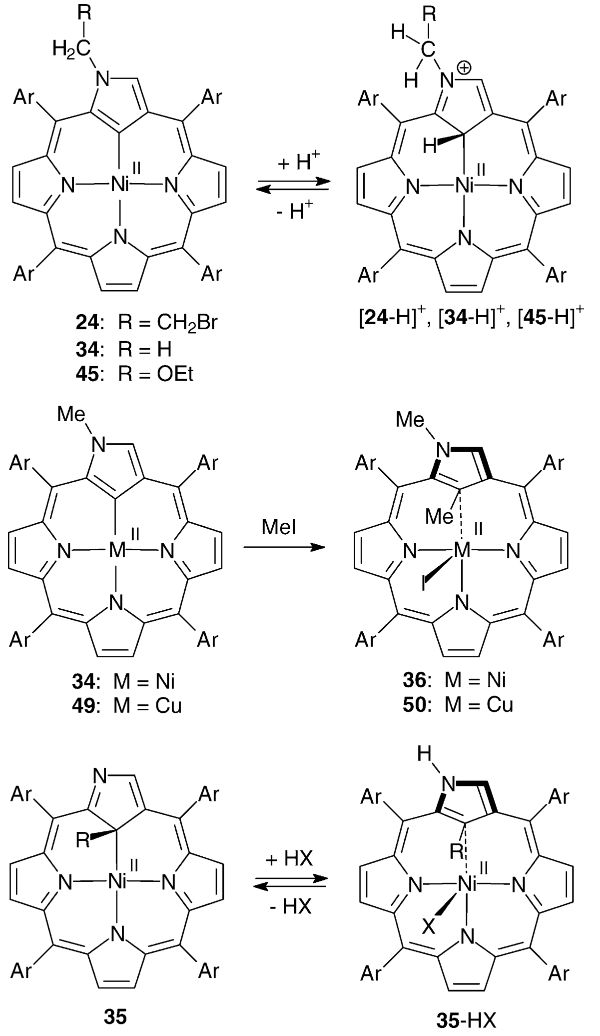

Scheme 28. Protonation and methylation of the alkylated NCP derivatives.

metal ion deprotonation allows chemical oxidation which affords EPR detection of a rare monomeric platinum(III) species (Fig. 11) [77]. Similar stabilization due to the deprotonation of 2-N has been observed for a copper(III) complex [67].

A high redox flexibility is observed for the 21-C-alkylated nickel(II) complex (**35a–d**). Their first oxidation potentials in the unprotonated form (500–700 mV versus SCE) are close to that of the unsubstituted complex (**18**) [94]. Generally chemical oxidation affords nickel(III) species which can be detected and characterized by EPR (Fig. 12, Table 3).

The trivalent nickel is slightly less stable after acidification since only an anodic shift of about 50 mV has been observed for the first oxidation potentials. In addition, a nickel(III) EPR signal can be still detected, even though it has different spin-hamiltonian parameters. On the other hand, after addition of an acid the reduction couple that appears at about −400 mV indicates the stabilization of the monovalent

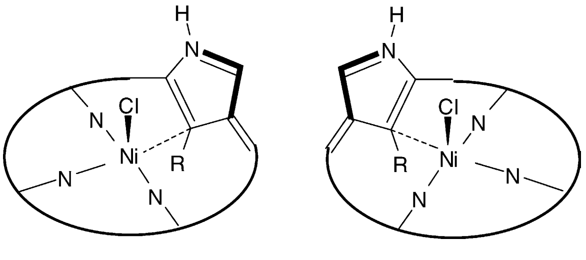

Scheme 29. Schematic representations of the enantiomers of 2-N-protonated 21-C-alkylated nickel(II) complexes of NCP.

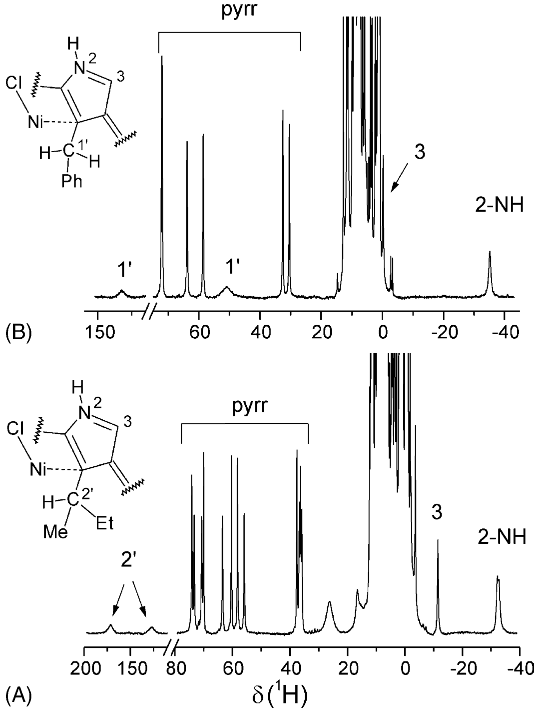

Fig. 9. ^{1}H NMR spectra (CDCl$_3$, 233 K) of paramagnetic nickel(II) complexes: (A) **35d**-HCl; (B) **35c**-HCl [94].

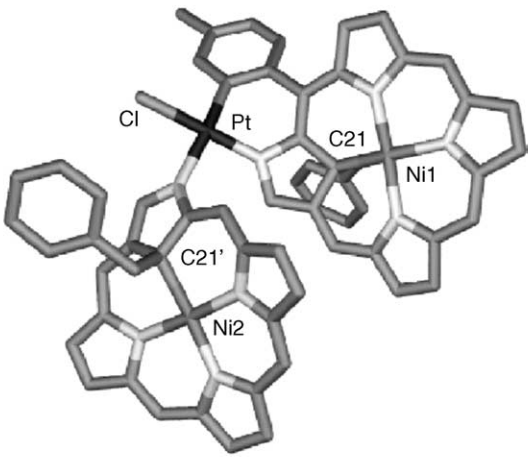

Fig. 10. A wire-frame representation of the molecular structure of the platinum(II)-linked dimer (**51b**) shows the asymmetric character of the compound and opposite configurations of the internal coordinated carbons 21 and 21′. All hydrogen atoms and all tolyl rings (with the exception of the orthometallated tolyl) are omitted for clarity [77].

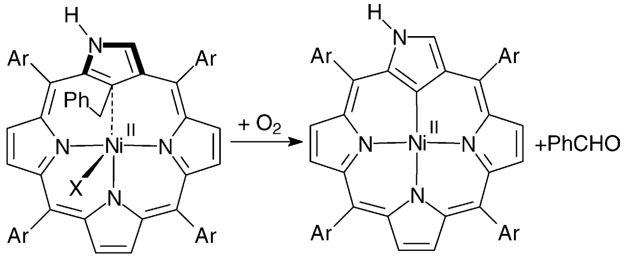

Scheme 30. Oxidative dealkylation of 21-C [94].

Table 3
EPR parameters[a] of selected nickel(III) complexes of NCP and its derivatives

Complex	L	g_1	g_2	g_3	g_{iso}	Reference
17	Cl^-	2.386	2.146	2.088	2.187	[74]
17	Br^{-}[b]	2.344	2.128	2.068	2.160	[74]
17	I^{-}[c]	2.275	2.115	2.035	2.138	[74]
17	NO_3^-	2.307	2.163	2.145	2.233	[74]
17	OH^-	2.274	2.190	2.109	2.193	[74]
56	Cl^{-}[d]	2.407	2.175	2.054	2.207	[94]
56	Br^{-}[e]	2.360	2.146	2.052	2.168	[94]
56	I^{-}[f]	2.305	2.127	2.040	2.169	[94]
39[g]	py	2.255	2.180	2.107		[97]

[a] Frozen solution spectra taken at 77 K, unless otherwise stated; isotropic parameters measured at 293 K.

[b] ^{79,81}Br hyperfine constants (in G): $A_1 = 23$, $A_2 = 3$, $A_3 = 126$, $A_{iso} = 55$.

[c] ^{127}I hyperfine constants (in G): $A_1, A_2 \sim 10$, $A_3 = 165$, $A_{iso} = 60$.

[d] ^{35,37}Cl hyperfine constants (in G): $A_3 = 25$.

[e] ^{79,81}Br hyperfine constants (in G): $A_1 = 30$, $A_2 = 40$, $A_3 = 124$, $A_{iso} = 59$.

[f] ^{127}I hyperfine constants (in G): $A_1 = 60$, $A_2 = 80$, $A_3 = 163$, $A_{iso} = 74$.

[g] Spectrum taken in frozen toluene at 130 K.

species, in line with a monoanionic character of the coordination core. Chemical reduction of the acidified system resulted in an EPR detection of a nickel(I) species (Fig. 12) [94].

Redox potentials also reflect the interaction between subunits in the oligomers of NCP. In the nickel(II) complex of the directly 3,3′-linked dimer (**23**) both oxidation and reduction couples are split, indicating an electrostatic influence of the charge appearing on one of the subunits on the potential of reduction/oxidation of the other subunit. (Fig. 13) [81]. The interaction between the subunits in the dimer is also reflected here by a larger (more than 300 mV) difference between oxidation and reduction potentials, with respect to the monomeric nickel(II) complex (**18**). In the methylene-linked dimers the influence of the subunits can be observed, despite the lack of electron density delocalization on the whole dimer. In the symmetric 2,2′-CH_2-linked nickel(II) complex (**44**) the first oxidation couple is split and so it is in the asymmetric 2,21′-CH_2 connected system (**43**) [94,99].

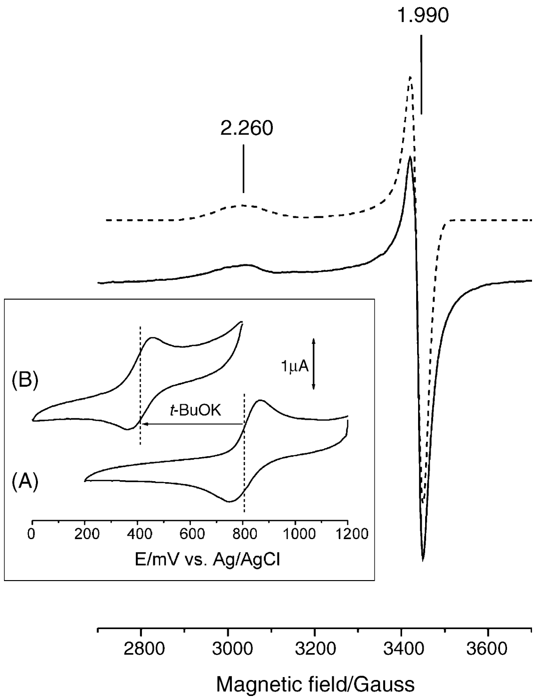

Fig. 11. Frozen solution EPR spectrum of the oxidation product of (NCP)Pt^{II} **21** by iodine in the presence of potassium *tert*-butoxide. Solid line – experimental spectrum, dashed line – simulated spectrum. Conditions: solvent, CH_2Cl_2/toluene mixture (50/50 v/v); temperature, 77 K; modulation frequency, 100 kHz; modulation amplitude, 5.5 G; microwave frequency, 9.58101 GHz; microwave power, 25.2 mW. Inset in the box shows first oxidation couples of platinum(II) complexes of inverted porphyrin: (A) **21**; (B) after addition of 3 equiv. of potassium *tert*-butyloxide in THF. Conditions: solvent, CH_2Cl_2, supporting electrolyte, 0.1 M TBAP; scan rate 100 mV/s; working electrode, glassy carbon disk; auxiliary electrode, platinum wire; reference electrode, Ag/AgCl (ferrocene reference, 530 mV) [77].

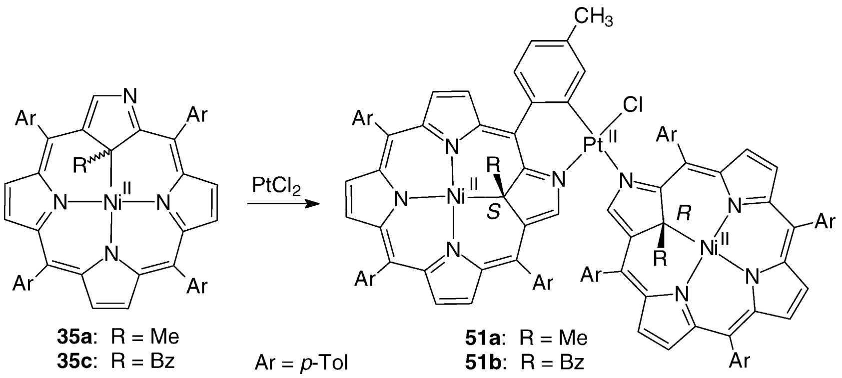

35a: R = Me
35c: R = Bz
Ar = *p*-Tol
51a: R = Me
51b: R = Bz

Scheme 31. Diastereoselective assembling of 21-C-alkylated nickel(II) NCP complexes on a platinum(II) [77].

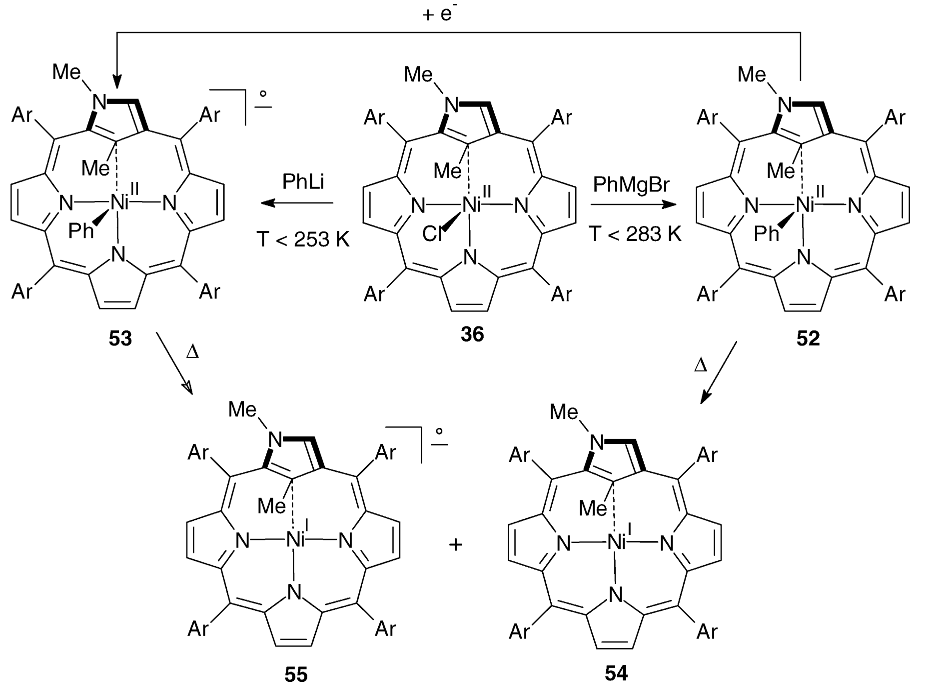

Scheme 32. Formation and decomposition of nickel(II) complexes with two different metal—carbon bonds [101].

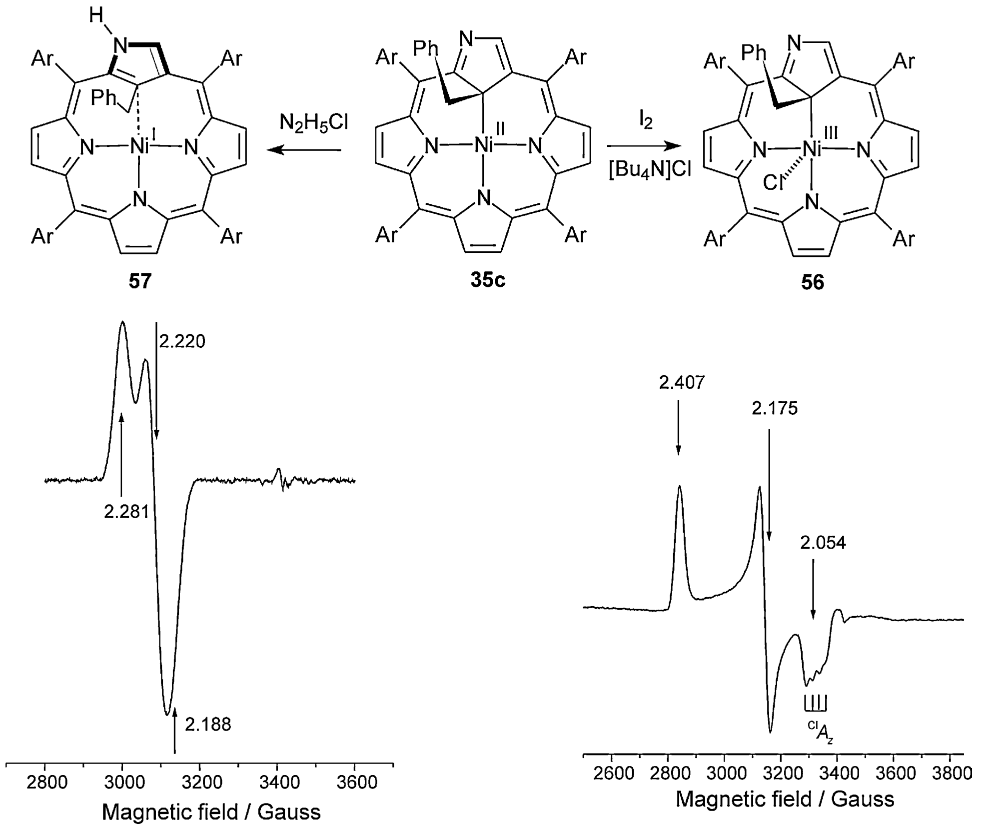

Fig. 12. Top: scheme of the redox processes for 21-benzylated nickel(II) NCP complex (**35c**). Bottom, left: frozen solution EPR spectrum of the 2-N-protonated complex upon reduction with hydrazine hydrochloride (**57**); right: frozen solution spectrum of the oxidized species (**56**) with marked hyperfine splitting due to an apical chloride coordination. Both spectra were taken at 77 K for toluene (**57**) or toluene/dichloromethane (**56**) solutions. The Zeeman parameters for both systems are marked with arrows [94].

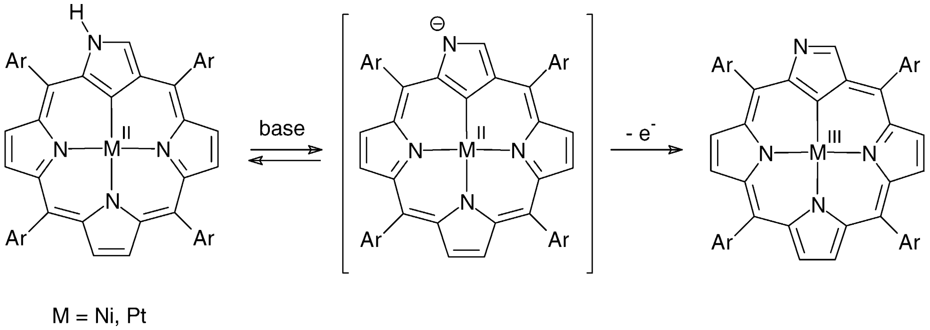

Scheme 33. Stabilization of a trivalent metal ion in the surrounding of NCP upon deprotonation of 2-N.

Although in the latter complex the appearance of two oxidation waves is due to a different environment of the nickel(II) ion in the subunits, their potentials are shifted to the higher values with respect to those of the respective monomeric methylated derivatives, i.e. **34** and **35a**, indicating an interaction between the metal centers. It is also possible that splitting of the oxidation and the reduction couples observed for the platinum(II)-linked asymmetric dimers (**51a**,**b**), containing two nickel(II) centers in a similar environment of the 21-alkylated NCP, is also caused by interaction between the subunits [77]. Interestingly, despite involvement of the external nitrogen in coordination in both subunits of **51**, there is no reduction couple that could be assigned to the Ni^{II}/Ni^{I} couple, analogous to that of the 2-N-protonated, 21-alkylated nickel(II) complexes.

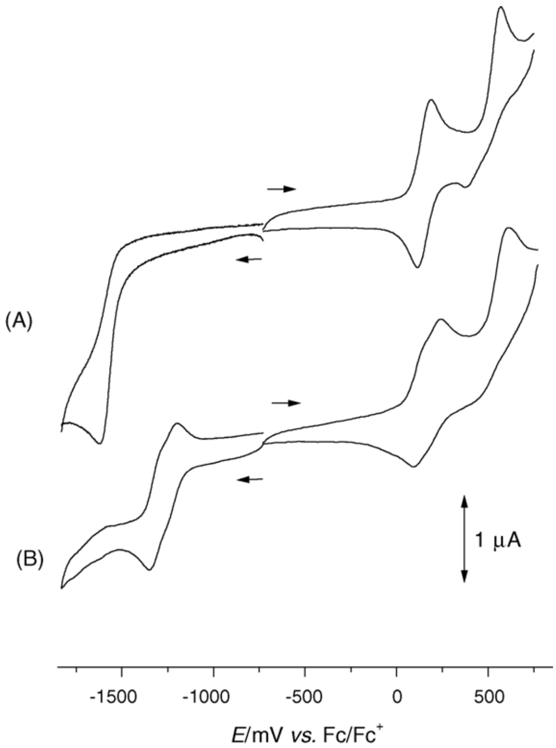

Fig. 13. Cyclic voltammograms of monomeric nickel(II) complex (**18**) (A) and a dimeric (**23**) (B) in CH_2Cl_2. Conditions: supporting electrolyte, 0.1 M TBAP; scan rate, 100 mV/s, working electrode, glassy carbon disk; auxiliary electrode, platinum wire; potentials referenced with Fc/Fc^+ at room temperature [81].

5. Conclusion

In this review we have demonstrated that alteration of the coordination core is a route of choice to stabilize unusual oxidation states and coordination geometries including such rare species as organometallic high-spin nickel(II) 21-heteroporphyrin or copper(II) 2-aza-21-carbaporphyrin [16–18,67,78,93].

In particular the porphyrin isomer, 2-aza-21-carbaporphyrin, the very first carbaporphyrinoid ever synthesized [1,2], continuously offers spectacular research opportunities, bringing together organometallic and macrocyclic chemistry. The coordination chemistry in the N-confused porphyrin environment takes advantage of the unique set of four donor atoms (NNNC) constrained in the porphyrin-like framework. Thus, this carbaporphyrinoid ligand enforces a coordination of a metal ion involving the inner carbon atom.

According to subsequent structural modification, direct σ-bonds of a trigonal or tetrahedral carbanion or side-on coordination have been discovered [93]. In any case, the adjacency of the metal and carbon atom provides an unprecedented route for activation of the carbocyclic moiety which is built into a metalloporphyrin-like structure. Clearly, N-confused porphyrin and its derivatives offer a non-trivial means to control properties of organometallic derivatives. The macrocyclic structure of an N-confused porphyrin allowed us to trap intermediates and frequently, elusive products of the metallocarbaporphyrinoid reactivity, which involves the metal ion–carbon atom moiety [73].

In the chemistry presented in this review there is much opportunity for future exploration in the organometallic direction outlined. To begin with, the properties of a variety of transition metal ions remain to be explored in the N-confused porphyrin setting. Alternatively, the *meso*-substituted macrocycles, which can be synthesized in numerous modifications, once one introduces a variety of carbocycles or heterocarbocycles are especially suited for exploration of intriguing aspects of organometallic chemistry, confined to the macrocyclic environment. For instance, the incorporation of the *meta*- or *para*-phenylene ring yields *meta*-benziporphyrin or *para*-benziporphyrin respectively [49]. Their properties can be fine-tuned to match particular purposes, for instance to activate arene C–H bonds, stabilize arene π-interactions with the metal, or generate unusual coordination modes in the macrocyclic core.

In more general terms, it remains to be seen how the nature of the inserted carbocycle or the choice of the metal ions influence the stability of the electronic and structural properties of metallocarbaporphyrinoids.

Acknowledgment

This work was financially supported by Polish Ministry of Scientific Research and Information Technology, grant 3 T 09A 162 28.

References

[1] P.J. Chmielewski, L. Latos-Grażyński, K. Rachlewicz, T. Głowiak, Angew. Chem. Int. Ed. Engl. 33 (1994) 779.
[2] H. Furuta, T. Asano, T. Ogawa, J. Am. Chem. Soc. 116 (1994) 767.
[3] K. Berlin, E. Breitmaier, Angew. Chem. Int. Ed. Engl. 33 (1994) 1246.
[4] T.D. Lash, Angew. Chem. Int. Ed. Engl. 34 (1995) 2533.
[5] L. Latos-Grażyński, in: K.M. Kadish, K.M. Smith, R. Guilard (Eds.), The Porphyrin Handbook, vol. 2, Academic Press, San Diego, CA, 2000, p. 361.
[6] T.D. Lash, in: K.M. Kadish, K.M. Smith, R. Guilard (Eds.), The Porphyrin Handbook, vol. 2, Academic Press, San Diego, CA, 2000, p. 125.
[7] H. Furuta, H. Maeda, A. Osuka, Chem. Commun. (2002) 1795.
[8] J.D. Harvey, C.J. Ziegler, Coord. Chem. Rev. 247 (2003) 1.
[9] We will use the symbol NCP for N-confused (inverted) porphyrin. Some modifications of the acronym are directly given in the text.
[10] A. Ghosh, Angew. Chem. Int. Ed. Engl. 43 (2004) 1918.
[11] P.J. Chmielewski, M. Grzeszczuk, L. Latos-Grażyński, J. Lisowski, Inorg. Chem. 28 (1989) 3546.
[12] L. Latos-Grażyński, J. Lisowski, M.M. Olmstead, A.L. Balch, Inorg. Chem. 28 (1989) 1183.
[13] L. Latos-Grażyński, J. Lisowski, M.M. Olmstead, A.L. Balch, Inorg. Chem. 28 (1989) 3328.
[14] P.J. Chmielewski, L. Latos-Grażyński, M.M. Olmstead, A.L. Balch, Chem. Eur. J. 3 (1997) 268.
[15] L. Latos-Grażyński, P.J. Chmielewski, New J. Chem. 21 (1997) 691.
[16] P.J. Chmielewski, L. Latos-Grażyński, Inorg. Chem. 37 (1998) 4179.
[17] E. Pacholska, P.J. Chmielewski, L. Latos-Grażyński, Inorg. Chim. Acta 273 (1998) 184.
[18] P.J. Chmielewski, L. Latos-Grażyński, Inorg. Chem. 31 (1992) 5231.
[19] B. Jaun, Metal Ions in Biological Systems, Marcel Dekker, New York, 1993.
[20] U. Ermler, W. Grabarse, S. Shima, M. Goubeaud, R. Thauer, Science 278 (1997) 1457.
[21] J.S. Lindsey, in: K.M. Kadish, K.M. Smith, R. Guilard (Eds.), The Porphyrin Handbook, vol. 1, Academic Press, San Diego, CA, 2000, p. 45.
[22] F.A. Walker, in: K.M. Kadish, K.M. Smith, R. Guilard (Eds.), The Porphyrin Handbook, vol. 5, Academic Press, San Diego, CA, 2000, p. 81.
[23] L. Latos-Grażyński, J. Lisowski, M.M. Olmstead, A.L. Balch, J. Am. Chem. Soc. 109 (1987) 4428.
[24] L. Latos-Grażyński, E. Pacholska, P.J. Chmielewski, M.M. Olmstead, A.L. Balch, Angew. Chem. Int. Ed. Engl. 107 (1995) 2252.
[25] L. Latos-Grażyński, E. Pacholska, P.J. Chmielewski, M.M. Olmstead, A.L. Balch, Inorg. Chem. 35 (1996) 566.
[26] E. Pacholska, L. Latos-Grażyński, Z. Ciunik, Angew. Chem. Int. Ed. 40 (2001) 4466.
[27] J. Lisowski, M. Grzeszczuk, L. Latos-Grażyński, Inorg. Chim. Acta 161 (1989) 153.
[28] L. Latos-Grażyński, M.M. Olmstead, A.L. Balch, Inorg. Chem. 28 (1989) 4065.
[29] P.J. Chmielewski, L. Latos-Grażyński, E. Pacholska, Inorg. Chem. 33 (1994) 1992.
[30] J. Lisowski, L. Latos-Grażyński, L. Szterenberg, Inorg. Chem. 31 (1992) 1933.
[31] M. Pawlicki, L. Latos-Grażyński, Inorg. Chem. 43 (2004) 5564.
[32] M. Pawlicki, L. Latos-Grażyński, Inorg. Chem. 41 (2002) 5866.
[33] K. Berlin, Angew. Chem. Int. Ed. Engl. 35 (1996) 1820.
[34] T.D. Lash, M.J. Hayes, Angew. Chem. Int. Ed. Engl. 36 (1997) 840.
[35] T.D. Lash, M.J. Hayes, J.D. Spence, M.A. Muckey, G.M. Ferrence, L.F. Szczepura, J. Org. Chem. 67 (2002) 4860.
[36] T.D. Lash, J.L. Romanic, M.J. Hayes, J.D. Spence, Chem. Commun. (1999) 819.
[37] T.D. Lash, S.T. Chaney, Angew. Chem. Int. Ed. Engl. 36 (1997) 839.
[38] T.D. Lash, Chem. Commun. (1998) 1683.
[39] S.R. Graham, D.A. Colby, T.D. Lash, Angew. Chem. Int. Ed. 41 (2002) 1371.
[40] M. Stępień, L. Latos-Grażyński, Chem. Eur. J. 7 (2001) 5113.
[41] M. Stępień, L. Latos-Grażyński, J. Am. Chem. Soc. 124 (2002) 3838.
[42] E. Pacholska, L. Latos-Grażyński, Z. Ciunik, Chem. Eur. J. 8 (2002) 5403.
[43] B.Y. Liu, C. Brückner, D. Dolphin, Chem. Commun. (1996) 2141.
[44] G.R. Geier III, D.M. Haynes, J.S. Lindsey, Org. Lett. 1 (1999) 1455.
[45] M. Stępień, L. Latos-Grażyński, T.D. Lash, L. Szterenberg, Inorg. Chem. 40 (2001) 6892.
[46] M. Stępień, L. Latos-Grażyński, L. Szterenberg, J. Panek, Z. Latajka, J. Am. Chem. Soc. 126 (2004) 4566.
[47] C.-H. Hung, F.-C. Chang, C.-Y. Lin, K. Rachlewicz, M. Stępień, L. Latos-Grażyński, G.-H. Lee, S.-M. Peng, Inorg. Chem. 4118 (2004) 4120.
[48] M. Stępień, L. Latos-Grażyński, L. Szterenberg, Inorg. Chem. 43 (2004) 6654.
[49] M. Stępień, L. Latos-Grażyński, Acc. Chem. Res. 38 (2005) 88.
[50] S.R. Graham, G.M. Ferrence, T.D. Lash, Chem. Commun. (2002) 894.
[51] M.A. Muckey, L.F. Szczepura, G.M. Ferrence, T.D. Lash, Inorg. Chem. 41 (2002) 4840.
[52] T.D. Lash, D.A. Colby, L.F. Szczepura, Inorg. Chem. 43 (2004) 5258.
[53] T.D. Lash, J.M. Rasmussen, K.M. Bergman, D.A. Colby, Org. Lett. 6 (2004) 549.
[54] T.D. Lash, D.A. Colby, S.R. Graham, G.M. Ferrence, L.F. Szczepura, Inorg. Chem. 42 (2003) 7326.
[55] H. Furuta, H. Maeda, A. Osuka, M. Yasutake, T. Shinmyozu, Y. Ishikawa, Chem. Commun. (2000) 1143.
[56] (a) H. Furuta, H. Maeda, A. Osuka, J. Am. Chem. Soc. 122 (2000) 803;
(b) H. Maeda, A. Osuka, H. Furuta, J. Am. Chem. Soc. 125 (2003) 15690.

[57] H. Furuta, H. Maeda, A. Osuka, J. Org. Chem. 65 (2000) 4222.
[58] M. Pawlicki, L. Latos-Grażyński, Chem. Eur. J. 9 (2003) 4650.
[59] N. Sprutta, L. Latos-Grażyński, Tetrahedron Lett. 40 (1999) 8457.
[60] C.-H. Lee, H.-J. Kim, Tetrahedron Lett. 38 (1997) 3935.
[61] E. Pacholska, L. Latos-Grażyński, L. Szterenberg, Z. Ciunik, J. Org. Chem. 65 (2000) 8188.
[62] A. Ghosh, T. Wondimagegn, H.J. Nilsen, J. Phys. Chem. B 102 (1998) 10459.
[63] H. Furuta, H. Maeda, A. Osuka, J. Org. Chem. 66 (2001) 8563.
[64] L. Szterenberg, L. Latos-Grażyński, Inorg. Chem. 36 (1997) 6287.
[65] J.D. Harvey, C.J. Ziegler, Chem. Commun. (2003) 2890.
[66] J.D. Harvey, C.J. Ziegler, Chem. Commun. (2004) 1666.
[67] H. Maeda, Y. Ishikawa, H. Matsueda, A. Osuka, H. Furuta, J. Am. Chem. Soc. 125 (2003) 11822.
[68] H. Furuta, T. Ogawa, Y. Uwatoko, K. Araki, Inorg. Chem. 38 (1999) 2676.
[69] T. Ogawa, H. Furuta, M. Takahashi, A. Morino, H. Uno, J. Organomet. Chem. 611 (2000) 551.
[70] J.-C. Liu, T. Ishizuka, A. Osuka, H. Furuta, Chem. Commun. (2004) 1908.
[71] H. Maeda, A. Osuka, Y. Ishikawa, I. Aritome, Y. Hisaeda, H. Furuta, Org. Lett. 5 (2003) 1293.
[72] D.S. Bohle, W.-C. Chen, C.-H. Hung, Inorg. Chem. 41 (2002) 3334.
[73] K. Rachlewicz, S.-L. Wang, J.-L. Ko, C.-H. Hung, L. Latos-Grażyński, J. Am. Chem. Soc. 126 (2004) 4420.
[74] P.J. Chmielewski, L. Latos-Grażyński, Inorg. Chem. 36 (1997) 840.
[75] H. Furuta, N. Kubo, H. Maeda, T. Ishizuka, A. Osuka, H. Nanami, T. Ogawa, Inorg. Chem. 39 (2000) 5424.
[76] H. Furuta, K. Youfu, H. Maeda, A. Osuka, Angew. Chem. Int. Ed. 42 (2003) 2186.
[77] P.J. Chmielewski, I. Schmidt, Inorg. Chem. 43 (2004) 1885.
[78] P.J. Chmielewski, L. Latos-Grażyński, I. Schmidt, Inorg. Chem. 39 (2000) 5475.
[79] I. Schmidt, P.J. Chmielewski, Tetrahedron Lett. 42 (2001) 1151.
[80] I. Schmidt, P.J. Chmielewski, Tetrahedron Lett. 42 (2001) 6389.
[81] P.J. Chmielewski, Angew. Chem. Int. Ed. 43 (2004) 5655.
[82] H. Furuta, T. Ishizuka, A. Osuka, H. Dejima, H. Nakagawa, Y. Ishikawa, J. Am. Chem. Soc. 123 (2001) 6207.
[83] P.J. Chmielewski, L. Latos-Grażyński, J. Chem. Soc., Perkin Trans. 2 (1995) 503.
[84] I. Schmidt, P.J. Chmielewski, Z. Ciunik, J. Org. Chem. 67 (2002) 8917.
[85] T.D. Lash, D.T. Richter, C.M. Shiner, J. Org. Chem. 64 (1999) 7973.
[86] J.D. Harvey, C.J. Ziegler, Chem. Commun. (2002) 1942.
[87] W.-C. Chen, C.-H. Hung, Inorg. Chem. 40 (2001) 5070.
[88] C.-H. Hung, W.-C. Chen, G.-H. Lee, S.-M. Peng, Chem. Commun. (2002) 1516.
[89] K. Rachlewicz, S.-L. Wang, C.-H. Peng, C.-H. Hung, L. Latos-Grażyński, Inorg. Chem. 42 (2003) 7348.
[90] H. Furuta, T. Morimoto, A. Osuka, Inorg. Chem. 43 (2004) 1618.
[91] H. Furuta, T. Ishizuka, A. Osuka, J. Am. Chem. Soc. 124 (2002) 5622.
[92] H. Furuta, T. Ishizuka, A. Osuka, Inorg. Chem. Commun. 6 (2003) 398.
[93] P.J. Chmielewski, L. Latos-Grażyński, T. Głowiak, J. Am. Chem. Soc. 118 (1996) 5690.
[94] I. Schmidt, P.J. Chmielewski, Inorg. Chem. 42 (2003) 5579.
[95] Z. Xiao, B.O. Patrick, D. Dolphin, Chem. Commun. (2003) 1062.
[96] Z. Xiao, B.O. Patrick, D. Dolphin, Chem. Commun. (2002) 1816.
[97] Z. Xiao, B.O. Patrick, D. Dolphin, Inorg. Chem. 42 (2003) 8125.
[98] C.-H. Hung, S.-L. Wang, J.-L. Ko, C.-H. Peng, C.-H. Hu, M.-T. Lee, Org. Lett. 6 (2004) 1393.
[99] I. Schmidt, P.J. Chmielewski, Chem. Commun. (2002) 92.
[100] A. Srinivasan, H. Furuta, A. Osuka, Chem. Commun. (2001) 1666.
[101] P.J. Chmielewski, L. Latos-Grażyński, Inorg. Chem. 39 (2000) 5639.